

# Haptic Surgical Guidance for Prostate Biopsy

BY

MARTINA BERNI

B.S, Politecnico di Milano, Milan, Italy, 2016

THESIS

Submitted as partial fulfillment of the requirements  
for the degree of Master of Science in Bioengineering  
in the Graduate College of the  
University of Illinois at Chicago, 2018

Chicago, Illinois

Defense Committee:

Cristian Luciano, Chair and Advisor

Craig Niederberger, Urology

Elena De Momi, Politecnico di Milano

*"Man cannot discover new oceans  
unless he has the courage to lose  
sight of the shore"*

Andre Gide

To my family, for making me feel close to home despite the distance.

## ACKNOWLEDGMENTS

I would like to sincerely thank my thesis advisor, Dr. Cristian Luciano, for his present support and guidance during the project. He stimulated and motivated me to do my best during the whole work, creating a pleasant working environment at Mixed Reality Lab, of which I would like to thank the members.

Besides my advisor, I would like to thank all the colleagues of the UR\*Lab and the Innovation Center for the feedback and technical support, and Dr. Craig Niederberger, as head of the Urology Department, also for the founding.

Moreover, I would to thank my Italian advisor, Dr. Elena De Momi, for her long-distance guidance role.

A profound thank you is for my parents, for their efforts, their motivation and their trust in my capabilities. I would like to thank my *coinqui*, Gre, Ele, Hope and Leo, for being my Chicago family. It was a pleasure coming home these months and find you: Ele, for the energy and sticky fruit label, Hope, for sens8 and the words of comfort, Gre, for being the best constant and mate of everything in these months full of blue line friends and free food, and Leo, for the open drawers and for being beside me along this experience. Many thanks to all the other Italians, it would not be the same without you.

Eventually, I would like to thank Paolo, Marta and Lorenzo for their support and encouragement, although the distance.

MB

## TABLE OF CONTENTS

<u>CHAPTER</u>	<u>PAGE</u>
<b>1 BACKGROUND . . . . .</b>	<b>1</b>
1.1 Prostate Anatomy and Physiology . . . . .	3
1.2 Prostate Cancer . . . . .	6
1.3 Prostate Biopsy . . . . .	10
1.4 Prostate Cancer Treatments . . . . .	17
1.5 Magnetic Resonance Elastography . . . . .	19
1.6 Haptic Medical Simulators . . . . .	21
1.7 Aim . . . . .	23
1.8 Thesis Structure . . . . .	25
<b>2 MATERIALS AND METHODS . . . . .</b>	<b>29</b>
2.1 Image Registration . . . . .	29
2.2 Hardware . . . . .	30
2.2.1 Design . . . . .	33
2.3 Software: LACE Library Description . . . . .	36
2.4 MRI, MRE and Histopathological Datasets Description . . . .	41
2.5 Implementation . . . . .	43
2.5.1 Reference System . . . . .	44
2.5.2 Volumes Representation . . . . .	44
2.5.3 Correction Sensor . . . . .	46
2.5.4 Registration . . . . .	47
2.5.5 Haptic Rendering on Volumes . . . . .	48
2.5.6 Haptic Guidance . . . . .	49
2.5.7 Graphical User Interface . . . . .	52
<b>3 CONCLUSION . . . . .</b>	<b>55</b>
3.1 Discussion and Conclusion . . . . .	55
3.2 Future Development . . . . .	56
<b>APPENDICES . . . . .</b>	<b>58</b>
<b>Appendix A . . . . .</b>	<b>59</b>
<b>Appendix B . . . . .</b>	<b>62</b>
<b>CITED LITERATURE . . . . .</b>	<b>67</b>
<b>VITA . . . . .</b>	<b>75</b>

## LIST OF FIGURES

<b><u>FIGURE</u></b>		<b><u>PAGE</u></b>
1	Male Reproductive and Urinary System Anatomy ( <i>Image courtesy of Katja Tetzlaff</i> ) . . . . .	4
2	Zones of the Prostate Gland ( <i>Image courtesy of Katja Tetzlaff</i> ) . . .	5
3	TRUS biopsy ( <i>Image courtesy of Katja Tetzlaff</i> ) . . . . .	11
4	Transperineal and Transrectal PBx . . . . .	12
5	Cores Location for Systematic PBx ( <i>Image courtesy of Katja Tetzlaff</i> )	14
6	Example of Liver MRE . . . . .	20
7	Example of simulators . . . . .	22
8	Proposed solution schema . . . . .	26
9	3D Monitor zoom . . . . .	26
10	Touch™ 3D Stylus by 3D System . . . . .	31
11	Ascension 3D Guidance® Specifications . . . . .	32
12	Shape connecting the biopsy needle to the haptic device . . . . .	33
13	Design of the base . . . . .	34
14	Plot of the obtained regression lines . . . . .	35
15	Hardware setup . . . . .	37
16	LACE Library Communication Workflow . . . . .	39
17	LACE Classes communication . . . . .	40
18	Overview of the application . . . . .	43
19	Application Interface . . . . .	45
20	Graphic User Interface . . . . .	48
21	Line Effect . . . . .	51
22	Target Visualization and Definition . . . . .	53
23	Graphic User Interface . . . . .	54

## LIST OF TABLES

<b><u>TABLE</u></b>		<b><u>PAGE</u></b>
I	TOUCH™ 3D STYLUS SPECIFICATION . . . . .	31

## LIST OF ABBREVIATIONS

2D	2-dimensional
3D	3-dimensional
AJCC	American Joint Committee on Cancer
AS	Ascension 3D Guidance®
BPH	Benign Prostatic Hyperplasia
CAS	Computer Assisted Surgery
CT	Computed Tomography
DCE	Dynamic Contrast-Enhanced Imaging
DoF	Degrees of Freedom
DRE	Digital Rectal Examination
DWI	Diffusion-Weighted Imaging
EMTS	Electromagnetic Tracking System
ERC	Endorectal Coil
FDA	Food and Drug Administration
GUI	Graphical User Interface
mp-MRI	Multi-Parametric Magnetic Resonance Imaging
MRI	Magnetic Resonance Imaging

## LIST OF ABBREVIATIONS (continued)

MRE	Magnetic Resonance Elastography
MRSI	Magnetic Resonance Spectroscopic Imaging
PBx	Prostate Biopsy
PCa	Prostate Cancer
CZ	Prostate Central Zone
PZ	Prostate Peripheral Zone
PSA	Prostate Specific Antigen
TNM	Tumor-node-metastases
TZ	Prostate Transition Zone
QH	QuickHaptics <sup>TM</sup>
T1-WI	T1-Weighted Imaging
T2-WI	T2-Weighted Imaging
TRUS	Transrectal Ultrasound
US	Ultrasound
VL	Visualization Library
VR	Virtual Reality
WK	Wykobi Computational Geometry Library

## SUMMARY

Prostate cancer (PCa), in addition to being the most widespread non-cutaneous cancerous form among American men, is the third prevalent factor of cancer-related mortality in the US. For this reason, early detection and accurate diagnosis are paramount for survival, increasing the possibilities of successful treatments.

Non-invasive screening tests are firstly performed and, if the presence of cancerous tissue is suspected, prostate biopsy is executed to assess the presence of malignant lesions inside the gland.

Blind systematic biopsy is the standard procedure allowing the extraction of cores through the guidance of transrectal ultrasound (TRUS) probe. This technique is inefficient and inaccurate because many samples must be taken in order to ensure some cores include cancerous tissue and small tumors might be missed. Whereas, if too many samples are extracted, the gland could be seriously damaged.

Targeted biopsy aims to improve detection rate and prevent oversampling. The most common guidance still relies on TRUS, while the target definition is based on magnetic resonance imaging (MRI). Limitations of this method resides in complexity and costs of the image fusion system.

The TRUS guidance in this thesis project is substituted by a real-time tracking obtained through the haptic device. Moreover, a *correction sensor* is placed on the patient pelvis to take into account possible movements.

## SUMMARY (continued)

The *haptic surgical guidance for prostate biopsy* main aim is to improve current prostate biopsy (PBx) procedure directing the surgeon toward the center of the tumors, identified with magnetic resonance elastography (MRE).

Through MRE, mechanical properties of the tissue are acquired and a 3D map with stiffness distribution is consequently obtained. This technique provides an innovative diagnostic tool and targeting methodology, because cancerous areas are stiffer respect surrounding healthy tissues. The mentioned property allows the identification of the center of the tumors through clustering techniques.

In the virtual reality (VR) environment, pre-surgical planning can be conducted through the visual and haptic feedbacks obtained interacting with the simulated prostate. Before the procedure, image registration is fundamental to match information from the different imaging techniques and also to create coherence with anatomical data. Finally, the surgeon is guided towards the identified targets, through the force feedback provided by the haptic device.

## CHAPTER 1

### BACKGROUND

PCa is the most widespread malignant lesion between American men, excepting skin tumor. The American Cancer Society appraises that about 1 male subjects in 9 will be recognized with cancerous cells in the prostate over his life, and a man in 41 will de cease of it. With 164,690 new estimated cases and 29,430 deaths, early detection and accurate diagnosis have a paramount role for survival[1].

Common screening tests for the detection of tumors in the prostate gland are digital rectal examination (DRE) and prostate specific antigen in blood (PSA), but these methods are not completely accurate.

Multiparametric Magnetic Resonance Imaging (mp-MRI) is increasingly been used during the last years. Although this technique may present limitations ranging from time and costs[2]. Moreover, tumors detection and staging is more reliable with larger dimensions and higher Gleason scores[3].

If cancer is suspected, prostate biopsy (PBx) is performed. It is considered the most accurate procedure to detect abnormal cells in the prostate gland. PBx consists in samples extracted through a hollow needle from various parts of the prostate and examined under the microscope. The gold standard is 12-core transrectal PBx, where samples extracted under the supervision of images obtained by a TRUS probe. However, more than 40% of PCas are isoechoic with the surrounding tissue and cannot be detected[4].

This method relies on sampling efficiency: many samples must be taken in order to ensure some of them include cancerous tissue. Systematic PBx is inaccurate because small tumors can be missed. A combination of these sampling errors can lead to false negative biopsy especially if under-sampling occurs. On the other hand, over-sampling can induce the detection of clinically insignificant disease and the prostate can be seriously damaged. The necessity for repetitive biopsy increases the risk of complications.

Higher accuracy could be achieved under the guidance of MRI-TRUS images, limiting the number of taken samples[5]. Since the US probe is still present, it causes deformation and displacements of tissues and surrounding structures and computationally heavier algorithms to face this problem.

Innovative solution proposed by the *Virtual Reality Navigation System for Prostate Biopsy* [6] relies on the electromagnetic tracking system (EMTS) for the instrument localization respect the target, which has to be accurately defined. With this setup implementation the unreliable information provided by TRUS probe are not required, thus pre-operative images can be used without real-time algorithms correcting deformations.

Recently, the mechanical properties of tissues are studied for the assessment of the presence and aggressiveness of tumors. PCa has shown to change the elasticity of the tissue thus it is harder than surrounding healthy areas.

MRE is a non-invasive imaging technique evaluating in-vivo tissues mechanical properties, like stiffness. Elastograms are provided analyzing shear waves and stiffer areas could be easily detected. Thus, MRE provides supplementary diagnostic information also about aggressiveness.

In the *haptic surgical guidance for prostate biopsy* application, information about mechanical properties obtained through MRE are exploited to create an interactive VR environment in which volumetric data can be explored.

The center of the tumors is detected considering stiffness values of the tissue, then a force constrain guides the surgeon toward this identified point.

Meanwhile the localization of the instrument is based on navigation systems principles and it is developed through the haptic device, functioning as a tracker and avoiding the TRUS probe. Thus, the aim of this research is to develop a guidance for the clinicians performing PBx that can increase accuracy, precision and efficiency of the current procedures.

### **1.1 Prostate Anatomy and Physiology**

Belonging to the reproductive and urinary systems of men, the prostate is a muscular gland. It is sited inside the body, inferiorly respect the urinary bladder in pelvic cavity. Due to high incidence of PCa, it is relevant from oncological perspective[7]. In the following sections prostate anatomy and physiology are explained, then detection and treatment of PCa is discussed.

#### *Anatomy*

Prostate gland is located in front of the rectum and just below the bladder, the organ storing urine. Its size is about the size of a chestnut and it constituted of one base, one apex, an anterior, a posterior and two lateral surfaces. While the base is located in proximity of the lower surface of the bladder and it is in continuity with bladder wall, the apex and the superior fascia of the urogenital diaphragm are in contact[8][9].

The prostate is composed of several types of tissue and it is divided into zones[10][11][12]:

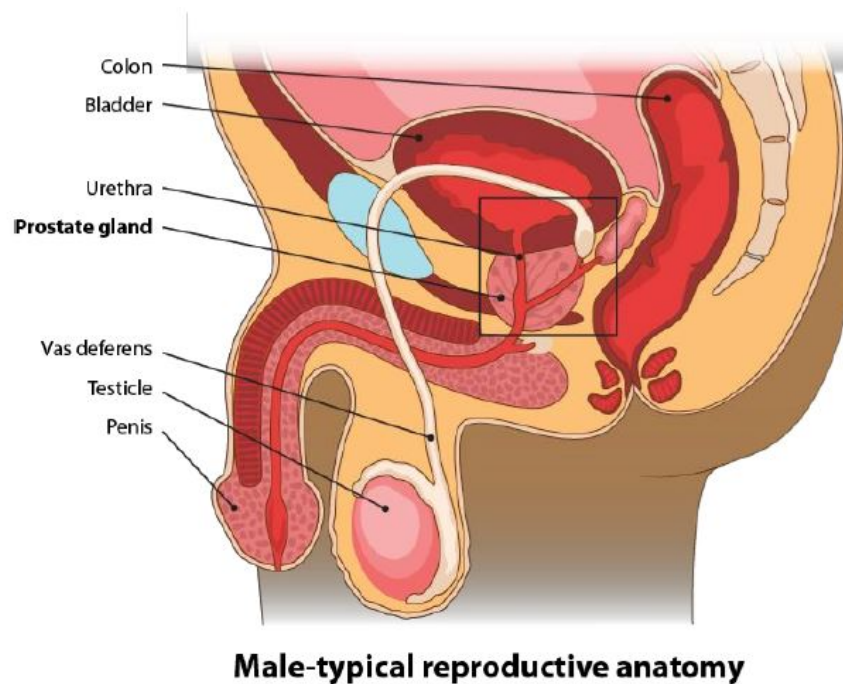


Figure 1: Male Reproductive and Urinary System Anatomy  
*(Image courtesy of Katja Tetzlaff)*

- Peripheral zone (PZ)

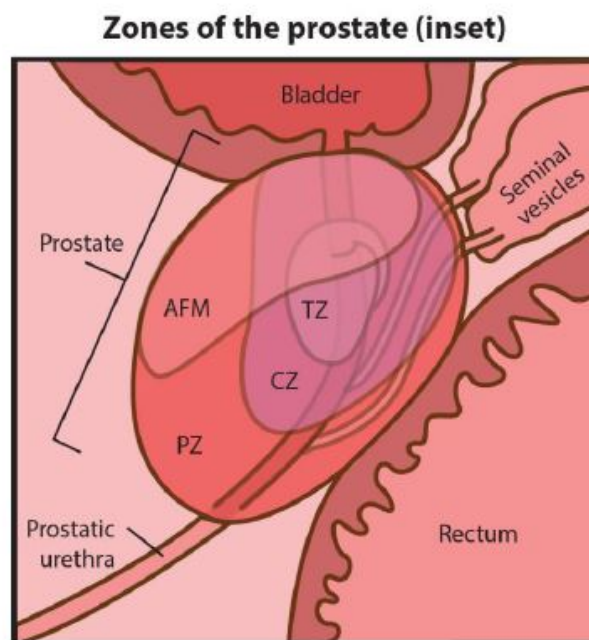
In the PZ, the majority of prostatic glandular tissue is contained and this zone is the closest one to the rectum, thus located at the back of the prostate. While DRE is performed, this is the zone which is felt. About 70/80% of PCa originate in PZ.

- Transition zone (TZ)

It is the area surrounding the portion of urethra passing through the prostate. The increase in size of this zone with men age is a condition called benign prostatic hyperplasia (BPH). The percentage of PCa beginning in this zone is about 20%.

- Central zone (CZ)

CZ surrounds the ejaculatory ducts, running from the seminal vesicles to the prostatic urethra. Less than 5% of PCa begins in the CZ, but this kind of tumors is more aggressive and there is more probability to invade the seminal vesicles.



AFM = Anterior fibromuscular zone  
TZ = Transition zone  
CZ = Central zone  
PZ = Peripheral zone

Figure 2: Zones of the Prostate Gland  
(Image courtesy of Katja Tetzlaff)

### *Function*

Both reproductive and urinary systems are influenced by prostate function. The main aim of the prostate gland is to produce prostatic fluid for semen, that allows the transportation of sperm during the male orgasm. This fluid is rich in enzymes, proteins and minerals nourishing the sperm. It also controls the urinary flow, since the urinary tract, starting from the bladder crosses, TZ of the prostate before the penis. Prostate muscles act the control on the urinary flow because they wrap the urethra. Through the contraction of these muscles, the flow is regulated[13].

## **1.2 Prostate Cancer**

Since the prostate gland surrounds the urethra, the diseases associated to this organ affects the efficiency of urinary system. While common problems are benign (noncancerous), like BPH, acute and chronic infections called prostatitis (bacterial or not), the PCa is a malignant condition in which DNA damages induce abnormal and uncontrolled cells growth. Accounting for about 95% of all PCa, Adenocarcinoma is the common type developing in the different glands zones. The complexity in prognosis and therapy increases when PCa grows as multifocal and this condition, according to researchers occurs within 60-90%[14]. Due to the high mortality rate, early detection and accurate diagnosis are paramount for survival.

### *Diagnosis*

In its early stages, PCa often does not cause any signs or symptoms. These conditions usually appear as soon as the tumor grows and causes changes in bladder functionality. For this reason,

common signs and symptoms include disturbs in the urination, which could be more frequent and urgent. The main early screening exams for PCa are PSA test, DRE and mp-MRI.

- PSA blood exam

The PSA blood test grades the amount of a protein created by cells of prostate gland and by possible malignant cells, in the blood. Its function is to keep the semen in liquid form. This test, originally approved by FDA in 1986[15], indicates an increased likelihood of PCa, if the PSA is changed significantly over time or is at an elevated level. Also, the rise of a man's PSA level can be attributed to non-cancerous conditions, like BPH or prostatitis. Furthermore, only 20% of PCa is identified in patients with a minor level of PSA. While in the past the threshold of PSA for further investigations was of level of 4.0 ng/mL, recent studies demonstrated that PCa occurs with lower levels. Moreover, several factors induce this level to oscillate. PSA examinations are tracked over time to detect any change; thus, the PSA velocity is the time that the PSA needs to increase. Both the velocity and the doubling time are used to determine the need of further tests. The PSA was approved by FDA in 1994 with the conjunction of DRE for screening.

- DRE

DRE consists in the insertion of the doctors gloved and lubricated finger into the rectum, with the aim to feel hard or abnormal areas in the prostate that may indicate PCa. In this way, the back portion of the gland can be felt. As mentioned previously, the drawback is that not all the tumors originate from the reachable PZ. Moreover, the majority of cancers detected through this technique alone are clinically or pathologically

advanced[16]. Despite this exam has been performed for long time, nowadays researches do not recommend it, both alone or in combination with PSA test. Due to the inherited limitations of this method, the positive predictive value ranges from 5% to 30%.

- TRUS

It is traditionally used to provide images of the prostate and one of the most common imaging technique, especially it provides guidance for brachytherapy and biopsies. Advantages of this imaging modality ranges from low costs, good availability to real time visualization. Despite the excellent contrast to distinguish the prostate, boundaries, anterior rectal wall, bordering bladder and seminal vesicles, the information obtained about the prostate tissues and benign or malignant lesions is not reliable or consistent. This because often (40%-60%) PCa are isoechoic, thus not visible with US. While, hypoechoic areas have the probability of being cancer in a range of 17-57%[4].

- mp-MRI

The accurate localization is increased by mp-MRI, an evolving noninvasive imaging technique. It combines the following imaging:

- T2-weighted imaging (T2-WI);
- diffusion-weighted imaging (DWI);
- spectroscopic imaging (MRSI);
- perfusion imaging;
- dynamic contrast-enhanced (DCE).

Higher SNR is achieved using 3T to obtain images, while endorectal coil (ERC) at 1.5T is suggested for staging purposes[17][18][19].

T1-WI (T1-weighted imaging) is mainly used in detecting post-biopsy hemorrhage, since the contrast generally provided is small.

T2-WI provides the highest spatial resolution, thus defining the different anatomical zones and outlining the neurovascular bundles. Since it reflects the water content, PZ is shown as a high intensity signal respect the PZ. The Gleason grade of the tumor is found to be correlated to this phenomenon. This means that lower the signal is, grater is the Gleason score. Similar responses could be also seen in presence of benign abnormalities; thus, the detection specificity is about 60%, while the sensitivity is good (about 80%)[20]. PCa aggressiveness is determined using a grading system: the Gleason score. It ranges from 1 to 5, with lower values from normal tissue and higher grade for abnormal one (usually  $\geq 3$ ). For each patient, two scores are assigned: one describing the cells constituting the largest area of the tumor and the other related to the cells of the following largest area. Grades up to 6 indicates cancer cells similar to normal cells, thus growing slowly. An intermediate risk is described by a score of 7, while Gleason values higher than 8 suggest PCa spreading rapidly.

DWI is an imaging tool probing the function of tissues, measuring the water molecules movements in tissues (Brownian motion)[21]. A reduced water diffusion is correlated to the increased malignant lesion. For these reasons, DWI is examined the dominant sequence for PCa recognition. Researchers affirm that the sensitivity is about 79%, while the

specificity 85%. DCE MRI is based on T1-WI and a contrast material. Obtained images can be evaluated both quantitatively and qualitatively, showing the vascular properties of tissues. Unlike T2-WI and DWI, investigations show low correlation between DCE MRI parameters and Gleason score. But this sequence allows to detect residual or recurrent tumors, leading attention to small foci. The sensitivity and specificity to detect malignancy are, respectively, of 89% and 90%[22]. From literature is shown that adding MRSI to MRI, the ability to detect PCa is improved because it considers metabolic information. Its clinical application is limited due to the required time and expertise. MRSI shows sensitivity and specificity of 89% and 69%, respectively[23].

If PCa is suggested from these screening tests, the standard care for more accurate detection of suspicious cells inside the prostate gland is PBx. During this procedure, through a core needle, small samples of tissue are removed and then analyzed under a microscope. Further and detailed description of PBx is presented in the following section.

### **1.3 Prostate Biopsy**

It is the gold standard for PCa diagnosis and it is performed after abnormal screening test results.

The urologist takes cores, small cylinders, of tissues from the prostate through an hollow needle and thanks to the guidance of images.

The needle used to perform biopsy is hollow, in order to capture specimen. A core needle, utilized for PBx, is composed by an inner needle coupled to a shallow receptacle, protected by a sheath and attached to a spring-loaded mechanism. This allows the surgeon to quickly extend

and retract the final portion of the needle capturing the core.

### *Access Point*

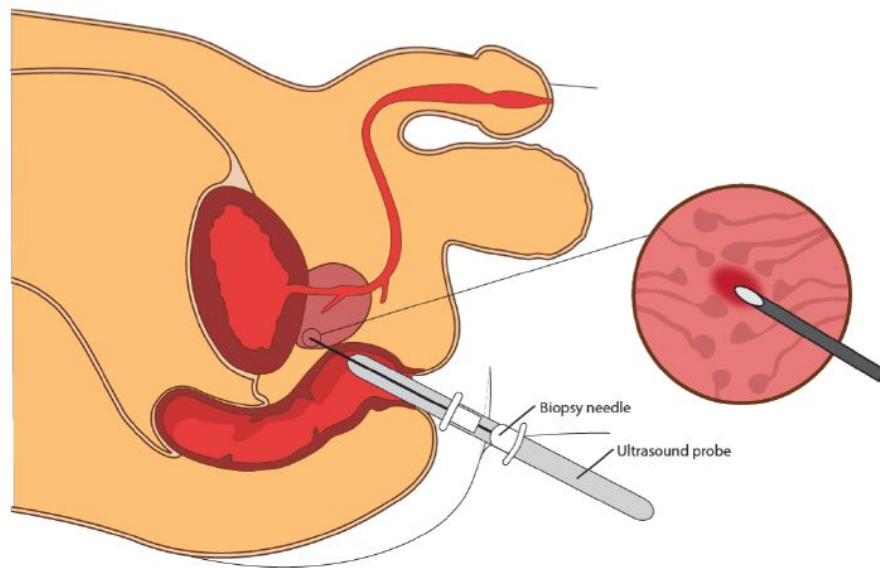


Figure 3: TRUS biopsy  
(Image courtesy of Katja Tetzlaff)

The prostate can be reached through the rectum, acting a transrectal PBx, or through the perineum, transperineal PBx.

Their main difference resides in the puncture site and puncture route[24][25].

In transperineal biopsy, the skin is punctured at the perineum and the prostate is reached parallel to the urethra; while with the other approach the insertion occurs through the anterior

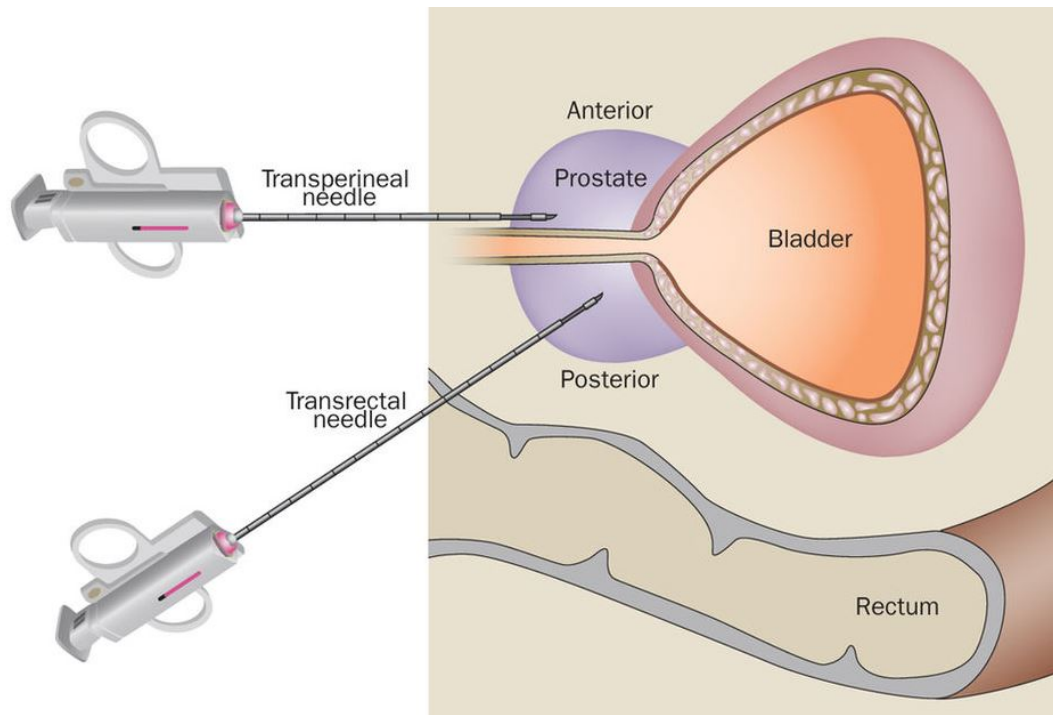


Figure 4: Transperineal and Transrectal PBx [25]

rectal wall[26].

Since PCa is shown to be more common in the peripheral and apical region of the prostate, transperineal PBx is preferred for the better sampling of these areas. However, the cancer detection rate has been demonstrated by several studies to be equivalent increasing the number of cores[27]. Transperineal PBx has drawbacks like time consumption, more complex and painful, and it requires an higher grade of anesthesia. On the other hand, infectious complications are obviously more frequent in the procedure performed through the rectum. Despite this, transrectal PBx is globally more popular than transperineal procedure.

In conclusion, researches discover that the cancer detection rate and complications are comparable in the two methods. The appropriate access point is evaluated considering the specific case.

### *Samples and Guidance*

Generally, PBx is performed after screening tests including images; thus, the ideal procedure is focused on extracting samples only from suspicious areas. This would lead to a reduction of discomfort and risks for the patient, and, mainly, the maximum accuracy.

The most common procedure for PBx, random systematic, is blind to the location of lesions. In fact, a fixed number of cores is randomly extracted from different areas of the prostate gland. Samples are taken randomly because usually it is executed under the TRUS guidance, thus not reliable in the definition of lesions, and because lesions in mp-MRI can be not recognized. This method for PBx is able to detect approximately 70% of PCa in the PZ, while considering the whole gland the percentage drops to 30%-40%[28][29].

With the aim to increment the cancerous lesions detection rate, there is an ongoing debate about the number of samples to be taken while performing PBx. Hodge et al. proposed in 1989[30] the sextant technique consisting in the collection of six samples at the base, middle third and apex of the gland, bilaterally respect to the sagittal plane. Because of 30% of results occurs in incorrectly identify as absent the PCa, more cores have been introduced.

The extended lateral PZ protocol (10-12 cores) presents from four to six lateral added samples respect the sextant one. This is the most common and preferred protocol, but more specimens could be taken in the TZ (from 2 to 3 for each side) or adding them in the midline.

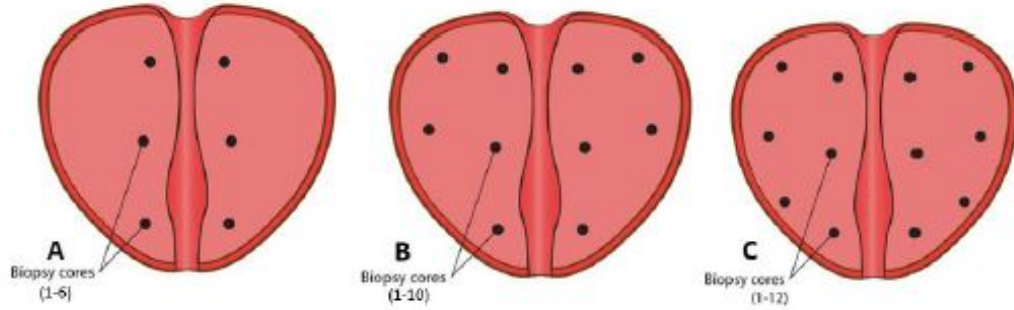


Figure 5: Cores Location for Systematic PBx  
*(Image courtesy of Katja Tetzlaff)*

From literature, studies related to the optimal number of cores results in dependencies on the group of patients considered[31]. Generally, an increased detection rate is not necessarily given by an augmented number of extracted samples, which, on the other hand, rises the risk of complications.

Hence, conventional biopsy relies upon improving sampling increasing the specimens with a tradeoff with complications; an alternative methodology is based on the reduction of errors through the suspicious lesions localization.

Since the aim is to diminish the amount of false negative results without oversampling the prostate gland during the PBx, targeting the biopsy toward the lesions detected through imaging techniques could be the solution.

From US images, hypoechoic areas consist in suspicious lesions that could be addressed while performing the PBx. In this case, the detection rate of PCa increases by 3.5% with a still limited sensitivity[32].

The limitations in specificity and sensitivity for prostate cancer detection using standard gray-scale TRUS leads to the investigation of alternatives. Doppler TRUS and Power Doppler imaging has been studied, but no significant information is added to gray-scale TRUS images. Color Doppler TRUS sensitivity for PCa detection ranges between 50% and 87%, with a specificity of 38%-93%. Using contrast elements the sensitivity is significantly improved, with a specificity of 80%; leading to the reduction of the number of samples. For the complexity, high costs and low specificity in distinguishing between benign and malignant lesions, this technique is not common.

MR-targeted biopsy has been developed because of the accurate localization of PCa given by mp-MRI. It is demonstrated that a lower number of PCa is detected compared to the systematic procedure, meanwhile the number of clinically significant cancers is similar[33].

The simplest method to use information given by MRI while performing PBx is the cognitive fusion, in which the surgeon integrates the information, thus depending on his capability[34][35]. During direct MRI-targeted PBx, the patient is in the MRI scanner and target is reached under MRI visualization, thus only the target is sampled. The drawbacks reside in costs and required time.

While in the US-MRI fusion biopsy, real time images are provided by US. The preoperative MRI are fused with real-time US images through a digital overlay. The reconstruction of the prostate consists in a 3D model created from the registration of the previous images with the current ones, taking into account the displacement introduced by the probe and possible movement of the patient. The targets, individuated in MRI, has to be consistent in the new volume.

Despite the use of familiar procedures, the computational cost are high, additional devices and training of specialized operators are requested[5][36].

The increase in computing power achieved in the last decays allowed the growth of Computer Assisted Surgery (CAS) though medical images. Basically, CAS are computational tools and surgical procedures used to plan, guide or perform operations, with the aim to define the optimal surgical strategy[37][38].

A navigation system is an advanced approach of CAS, with more focus on information related to the localization of surgical instruments respect a target on a computer display. The aim is to allow the surgeon to plan the pathway of the instrument tip towards the target inside the patient, thus providing correspondence between the physical space, in which patient and instruments are located, and the virtual space with the images.

Firstly, images are acquired, then pre-processed to take into account possible geometric distortions caused by patient motion. The following step involves the segmentation of the image to identify region of interest (ROI). Where appropriate, this operation could superimpose different images of the same ROI to recognize the target.

To compute these procedure, medical image registration is necessary. It is the geometrical alignment of different images or volumes, in order to match the same anatomical structure in voxel coming from different image modalities or instruments.

Through tracking systems, the surgical tools are tracked and information about their location and orientation is given in real-time. EMTS are more precise and consequently more widely used in clinical practice.

The *virtual reality navigation system for targeted biopsy*[6] is an innovative prototype to perform transperineal targeted biopsy with the guidance of virtual images, obtained combining pre-operative MRI and a virtual needle tracked through EMTS. Preliminary evaluations report it as an intuitive method for targeted biopsy, allowing the elimination of TRUS, thus it can improve accuracy and safety of the procedure.

#### *Pain and complications*

PBx has also to be evaluated in terms of associated pain and complications for the patient. Despite it is minimally invasive, PBx is a painful procedure because of the multiple punctures made with thick biopsy needles. Since the cumulative nature of the pain, increasing the number of cores leads to increase the felt pain. Furthermore, the US probe insertion induces a mechanical stretch of the un-relaxed anal sphincter. Though periprostatic nerve block, i.e. local anesthesia, pain can be reduced[39].

On the other hand, complications can be linked to several factors, like the experience of the operator. Most common resulting problems are hematuria, rectal bleeding, pain in hypogastrium, urethra or perineum and retention of urine[40].

### **1.4 Prostate Cancer Treatments**

Once the PCa is diagnosed, determination of its stage has to be performed in order to characterize dimensions, aggressiveness, and expansion of cancer[1].

Universally adopted as system for stage PCa is the AJCC TNM system. T category describes the expansion of the prime tumor, N the possible spreading to nearby lymph nodes and M whether metastases are extended to other sites.

The stages are expressed with Roman numbers from I to IV, where lower stages cancers are less aggressive and with lower risk of recurrence after treatment than higher stages. Thus, stage I and II appears as localized PCa, stage III is locally advanced PCa, while the highest stage represents metastatic PCa. Staging is based on PSA level, Gleason score and tumor extension and it helps the urologists to choose the most effective treatment.

In medical decision making, patient preferences and values are acquiring importance since recent studies demonstrate an association with health outcomes. Thus, shared decision making is a collaborative process involving patients and clinicians that make decisions together[41]. Nowadays, the available options are the following[42]:

- Active Surveillance

It is a monitoring for PCa progression while not undergoing definitive therapy, thus involving PSA tests, physical examinations and/or PBx. Through this kind of surveillance is a feasible preference if the cancer is limited and improbable to expand quickly, once the disease is significantly developed more effective treatment is needed, like surgery and radiation. From literature, it is shown that the risk of metastasis and PCa mortality ranges from 0% to 6%, hence supporting the utility of this approach.

- Radiation Therapy (RT)

In this procedure, cancer cells are destroyed using X-rays. Two forms of RT could be performed: external beam radiation and brachytherapy. The first type of RT involves X-rays directed to the pelvis, while in the latter a radioactive source is placed into the

prostate gland. This second approach allows a more accurate targeting, reducing problems related to urinary tract and rectal discomfort.

- **Hormone Therapy**

Since androgens fuel the growth of PCa, treatments decreasing the levels of male hormones (androgen deprivation therapy) allow to reduce the volume and the advancement velocity of PCa.

- **Prostatectomy or Radical Prostatectomy**

It is a surgery performed removing the gland and surrounding tissues (seminal vesicles and lymph nodes) and reconnecting the urethra and the bladder. This procedure is chosen when cancer is limited to the prostate. Both open and laparoscopic surgeries are performed, moreover laparoscopic prostatectomy could be directly completed by the surgeon or assisted by robots. Common complications are urinary incontinence and erectile dysfunction.

## **1.5 Magnetic Resonance Elastography**

To evaluate in-vivo tissues mechanical properties, like stiffness, imaging technique is developed. This non-invasive approach is based on the characterization of biological tissue by assessing its response to deformation, thus also called remote palpation. This technique is sensitive to pathological changes, it has the potential to serve as an early diagnostic, non-invasive tool for multiple diseases[43][44][45].

Elastograms are provided analyzing shear waves and stiffer areas could be easily detected. Thus, MRE provides supplementary diagnostic information also about aggressiveness.

MRE allows the quantitative evaluation of the shear modulus of tissues, i.e. stiffness, through the analysis of waves propagation. Shear waves with a frequency in the acoustic range (20-500 Hz) are induced by an external vibration source and, while propagating, produce displacements perpendicular to the direction of wave propagation. Thus, the wave speed is related to the wavelength and frequency ( $c=\lambda f$ ) and stiffness is defined as  $\rho c^2$ , with  $\rho$  representing density.

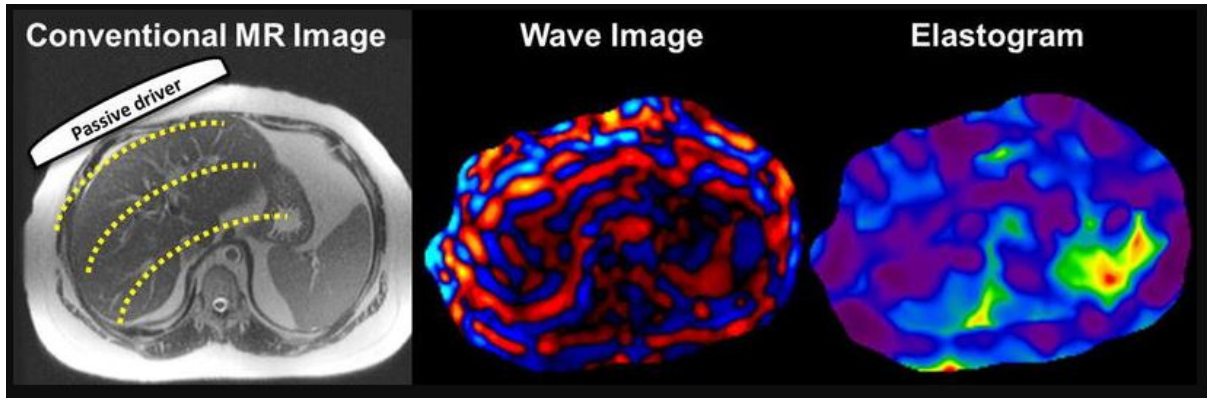


Figure 6: Example of Liver MRE [45]

The MRI phase images are obtained through motion-encoding gradients (MEGs) then the mechanical parameters used to generate elastograms are obtained with an inversion algorithm.

Focusing on the prostate gland, several studies, both ex vivo and in vitro, have shown that the resulting stiffness measures are different between malignant PCa and benign lesions or normal

tissue. This because the collagen deposition is increased in malignant lesions respect to normal areas.

MRE for cancer diagnosis, disease staging and spatial localization is an emerging application, currently limited because of the required time.

## **1.6 Haptic Medical Simulators**

There are several reasons inducing the spreading of medical simulators, e.g. patient safety, ethical issues, training and pre-operation planning. Moreover, VR permits to have multiple and exchangeable scenarios, environments that can be fully controlled, unlimited repetitions and automatic evaluation[46].

In fact, it is possible to simulate many complex medical procedures in a rapid, economic and realistic way. With the aim to increase realism, the most important non-visual modality is the haptic sensation, i.e. the reproduction of the tactile or force feedback. This because the success of many medical procedures depends on haptics cues and many researches have demonstrated their benefits in medical training through simulation. This is especially related to minimally invasive surgery procedures, which involve the touch, feeling and manipulation of organs through instruments[47].

Current studies will integrate haptics also in tele-diagnosis and telesurgery, in which the master robot provides forces to the surgeon resulting from the interaction of the slave robot and the patient [48].

Regarding PCa surgeries, examples of simulators without tactile feedback are the Robotic Surgical Simulator™ (Simulated Surgical System LLC™) and the da Vinci Skill Simulator (Intuitive

Surgical®Inc.).

DA VINCI SKILLS SIMULATOR  
Intuitive Surgical® Inc.



ROBOTIC SURGICAL SIMULATOR™  
Simulated Surgical System



Figure 7: Example of simulators

Systems incorporating haptic feedbacks are diagnostic tools like the robotic trainer rectum developed by the Imperial College of London. With this simulator a DRE is replicated, the users finger is inserted into a silicon rectum in which robotic actuators provide the tactile feedback replicating the modeled prostate on the screen[49].

The VR simulators for PCa mainly relies on MRI or CT images[50], while the introduction of MRE could straightforwardly lead the introduction of haptic cues based on the different

stiffness of the gland.

From literature, not many samples are found relating haptics and elastography, especially related to PCa.

There are some examples of haptic sensor with actuator able to visualize and reconstruct mechanical properties through US-elastography or using haptic devices[51][52]. During these studies, real-time strain imaging systems that allow tumor diagnosis and force investigation was developed. The potentiality of elastography is to increase the fidelity of the haptic feedback since it is not based on subjective evaluation.

Related to MRE, SenseViewer[53] was implemented to provide haptic, visual and auditory cues in medical images. The realistic tactile feedback is indeed obtained through MRE. Limitation of this device is that it has been developed for 2D medical images.

Since MRE offers the potential of implement accurate information about location and size of PCa in a non-invasive way, a useful tool is *Visuo-Haptic Model of Prostate Cancer Based on Magnetic Resonance Elastography*[54]. It offers a VR environment with a 3D model of the prostate gland based on MRE that could be explored through a haptic device. It is designed to improve pre-surgical planning, allowing the users to detect, assess and stage PCa in a non-invasive way, in the preliminary studies.

## 1.7 Aim

In section 1.3, there is a description of existing techniques to perform PBx. Due to the recent improvements of mp-MRI, the reached high sensitivity allows this imaging technique to significantly detect PCa (sensitivity and specificity respectively of 88% and 74%).

Through mp-MRI, location of suspicious lesions is determined and this definition allows to target the PBx. Studies have demonstrated that the number of individualized PCa is the same respect standard procedure, however the number of samples is lower and there is a strong reduction of insignificant cancer diagnosis.

From these results [55][56], there is evidence in the need of performing targeted biopsy, for the purpose of reducing oversampling and consequent risks of complications.

Image registration between pre-operative MRI and real-time TRUS has to be performed because the instrument position has to be tracked while performing the procedure. Since the US probe induces deformations and displacements of several structures, this process of image registration has an high computational cost and it is often inefficient because deformations cannot be perfectly reproduced in the virtual model[57].

TRUS caused discomfort and pain for the patient and it is not reliable for PCa detection since often tumors are isoechoic. Its role during targeted TRUS-MRI biopsies is to track real-time the instrument and the deformations induced by the probe. Thus, eliminating the US guidance another tracker is needed, like an EMTS as proposed in [6].

On the other hand, tissue elasticity provides a complementary information respect mp-MRI and it could lead to improvement in identification, localization and staging of PCa. As already mentioned, stiffness varies between normal tissue or benign lesion and malignant tumors. Furthermore, applications of 3D MRE provide more accurate mechanical properties estimations facing the limitations of 2D imaging.

The quantitative information acquired could be used to discriminate significant and insignif-

icant lesions through the determination of threshold values. Despite being proved that not all cancerous lesions are stiffer than normal tissue, the sensitivity obtained is of 86% and the specificity increases to 52% [58].

Consequently, information obtained through MRE allows to recreate a haptic feedback. It is thought to be essential for good clinical practice, especially for minimally invasive surgery [59]. The haptic or force feedback is, in this situation, linked to the sense of touch that the clinician experience while operating. Also in terms of training it is fundamental to obtain better and faster performances [60]. If no tactile response is provided, the surgeon experience difficulties in exerting the correct amount of force, especially on soft tissues, with a possible damage. Consequently, it is reported that addition of haptics reduces surgical errors and potentially can increase patient safety. Meanwhile, adding the sense of touch to the volume visualization increases the information captured about structure, location and consistence.

Systematic and random errors are made by humans while executing movements. They are caused by biases between visual estimates and proprioceptive information.

In haptic shared control, the assisting system control the human operator movements through forces and its benefits are proved [61]. In fact, the reaching of a target is improved with haptic guidance provided in an intuitive way [62].

## **1.8 Thesis Structure**

Facing the problem previously discussed, the proposed solution is a *haptic surgical guidance for prostate biopsy* in which the haptic feedback provided to the surgeon consist in a guidance towards identified tumors.

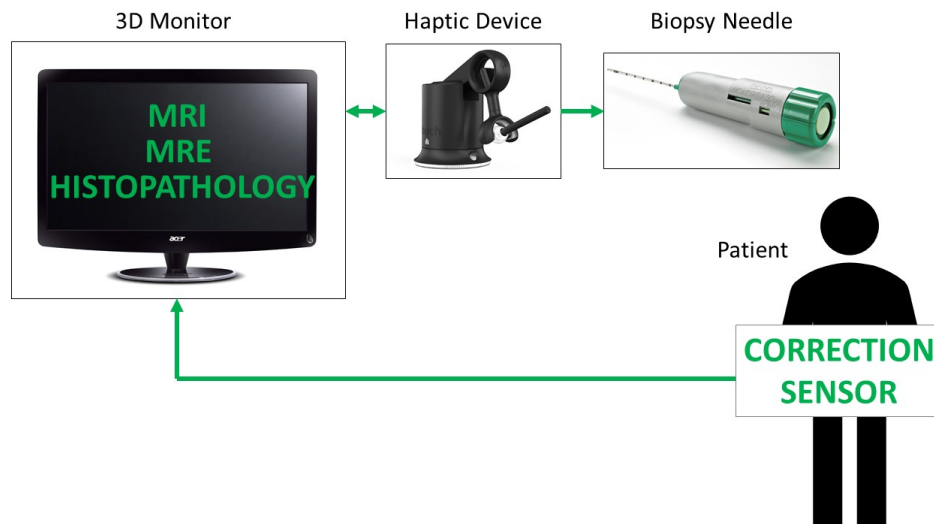


Figure 8: Proposed solution schema



Figure 9: 3D Monitor zoom

The displayed environment result from pre-operative MRI, ex-vivo MRE and histopathological images of three patients while the needle tracking is obtained through the haptic device.

The schema of the system is displayed in Figure 8.

From medical images, 3D volumes are obtained and registrations between them and the different related environments has to be performed. Then, during the procedure a *correction sensor* tracks through an EMTS possible displacements of the patient pelvis, while the needle position and orientation is attained given the haptic device stylus. This last equipment allows an enhanced tactile feedback resulting from MRE information. Whereas, the visual feedback is given through a virtual reality environment.

#### *Volumes and haptic feedback*

Imaging techniques allow to obtain volumetric representations of the patient. Merging information given by mp-MRI and MRE should allow to localize, size and stage in a more accurate, efficient and precise way PCa. While volumes reconstructed from histopathological images allow a first evaluation of the system.

The 3D model of the prostate gland is given by elastography, thus encoding mechanical properties that are perceived during its exploration through the haptic device.

#### *Tracking and Correction*

Being a development of a navigation system, the instrument has to be tracked real-time. This requirement allows to obtain the localization of the needle respect to the whole pelvis, the prostate gland and the target point. To acquire 3D location and orientation of the biopsy needle, the stylus of the haptic device is used. This is aimed to replace the TRUS, for its

limitation already described in section 1.3.

For what concern the correction of intra-operative prostate displacements, a *correction sensor* is placed on the patient pelvis continuously updating its position.

### *Registration*

Registration procedure allows to match anatomical information of the patient and the images in the virtual environment. This is performed through a paired-point registration, allowing the determination of the transformation matrix.

Other registrations were required for consistency while designing the whole system and will be described in the following chapter.

### *Performing Biopsy*

The centers of the tumors are obtained through clustering techniques, comparing MRE volumes with histopathological ones. While performing PBx with this system, the surgeon is haptically and visually guided toward these individuated points.

The main purpose of this project is to develop a guidance helping the surgeon to reach the center of the tumors individualized through clustering techniques. This, with the fusion of different imaging techniques and navigation system principles, aims to increase accuracy in detecting malignant lesions, efficiency in avoiding over-sampling of the gland, sensitivity and specificity of PCa recognition, and precision in detecting the center of the tumors. At the same time, it has to be easy to be performed by surgeon and safe for the patient and the clinician.

## CHAPTER 2

### MATERIALS AND METHODS

Since the inaccuracy, inefficiency and imprecision in localize and stage PCa through current PBx, this works aims to develop a system that easily grants the urologist to identify the centers of the tumors. For the correct planning and performance of the procedure, the virtual environment shows volumetric images of the patients. From the mechanical properties given by MRE, the haptic feedback is provided to the surgeon as an additional tool for capturing information, enhancing the characteristics of the tissues. Through registration the virtual scene is matched with anatomical information and the haptic and visual guide leads the surgeon toward the computed centers of the tumors.

In order to develop this, the volumes have to be firstly recreated from images focusing on the registration between all of them. Then hardware and software was implemented integrating the different information provided by the virtual environment, haptic device and EMTS.

#### **2.1 Image Registration**

Coherency must be achieved in order to create a virtual environment with a common coordinate system. The image registration is the process in which images or volumes are geometrically aligned overlapping common features, thus introducing a special transformation. It is needed when images are collected at disparate times either using different equipments[63].

Rigid image registration is computed through rotation, translation and scale of one image re-

spect the other to achieve correspondence. On the other hand, non-rigid registration is used to take into account deformations requiring stretching of the images.

B-spline registration is an image-based registration algorithm, aimed to precise match voxel by voxel[64]. It is one of the most common method for its general applicability, computational efficiency and because the perturbation of one control point is only reflected in its immediate neighbors[65].

To reduce the computational time required by MATLAB® in performing registration, 3D Slicer is used [66]. It is an open-source software from Kitware, Inc (Clifton Park) allowing image processing and 3D visualization. It was built on ITK [67], thus providing tools for both segmentation and registration, ranging from rigid/non-rigid to image-based/feature-based methods[68]. 3D Slicer provides a simple and intuitive way to perform B-spline registration of the whole set of images for each patient, thus creating consistency in the reference system.

## **2.2 Hardware**

The hardware is composed by the haptic device on which is attached the biopsy needle and the EMTS, both placed on a base, while the 3D Monitor displays the virtual environment. The used haptic device is Touch™ 3D Stylus, provided by 3D Systems Geomagic®[69], displayed in Figure 10. Specifications are summarized in the Table I.

During the development of this project the EMTS is produced by Ascension Technology Corporation[70]. It is composed by the following elements:

- a DriveBAY™: it is used to connect the transmitter and sensor to the computer. It is designed to fit in the computers drive bay and to perform a fast tracking;

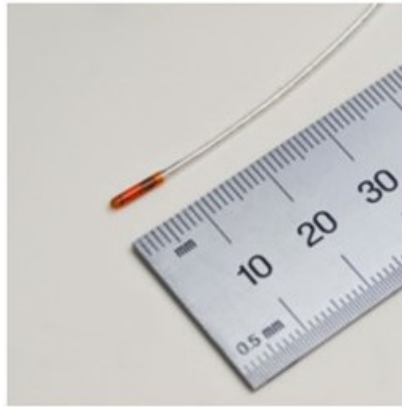


Figure 10: Touch™ 3D Stylus by 3D System

TABLE I: TOUCH™ 3D STYLUS SPECIFICATION

Type	Touch 3D Stylus
Positional Feedback	6 (Complete pose)
Force Feedback	DoF 3 (position only)
Force Feedback Workspace (WxHxD)	10.45x9.5x3.5"
Maximum Force	3.4 N
Nominal position resolution	0.084 mm

- a Mid-Range Transmitter: it covers larger anatomical regions than the Short-Range Transmitter. Its maximum tracking distance is of 660 mm;
- a Sensor: Model 130, used as a *correction sensor*. It measures intra-operative displacements and it should ideally be located in the position with maximum correlation between skin and prostate displacements.



MODEL 130	
Sensor OD	1.5 mm
Cable OD	1.2 mm
Sensor Length	7.7 mm
Cable Length	3.3 m

Mid-Range Transmitter	
Max Tracking Distance	660 mm in Normal Mode
Dimensions	96x96x96 mm
Weight	2.3 Kg



DriveBay™	
Number of sensors	Four 6DOF per unit
Measurement Rate	80 Hz default User configurable 20-255 Hz
Dimensions	180x147x41 mm
Weight	0.84 Kg
Interface	USB

Figure 11: Ascension 3D Guidance® Specifications

The 3D computer screen could be used, with special glasses, to enhance the 3D perception of the visualized models.

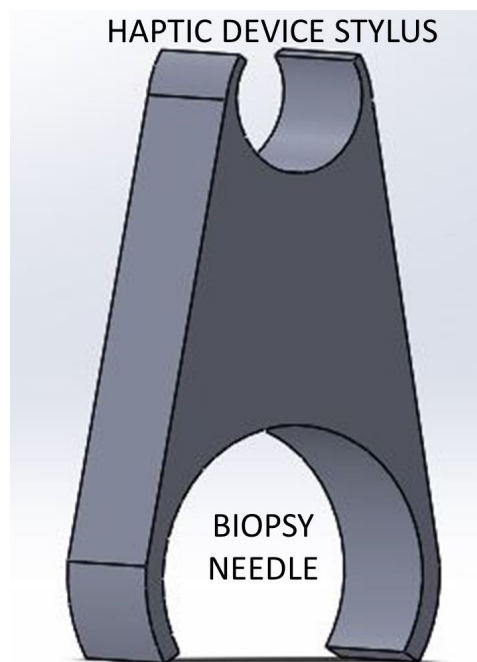


Figure 12: Shape connecting the biopsy needle to the haptic device

### 2.2.1 Design

The biopsy needle is attached to the haptic stylus through the 3D printed shapes, which are designed in SolidWorks™ (Dessault Systmes, Waltham MA)[71] shown in Figure 12.

Also the base is 3D printed (Figure 13), it allows to have a fixed relative position between

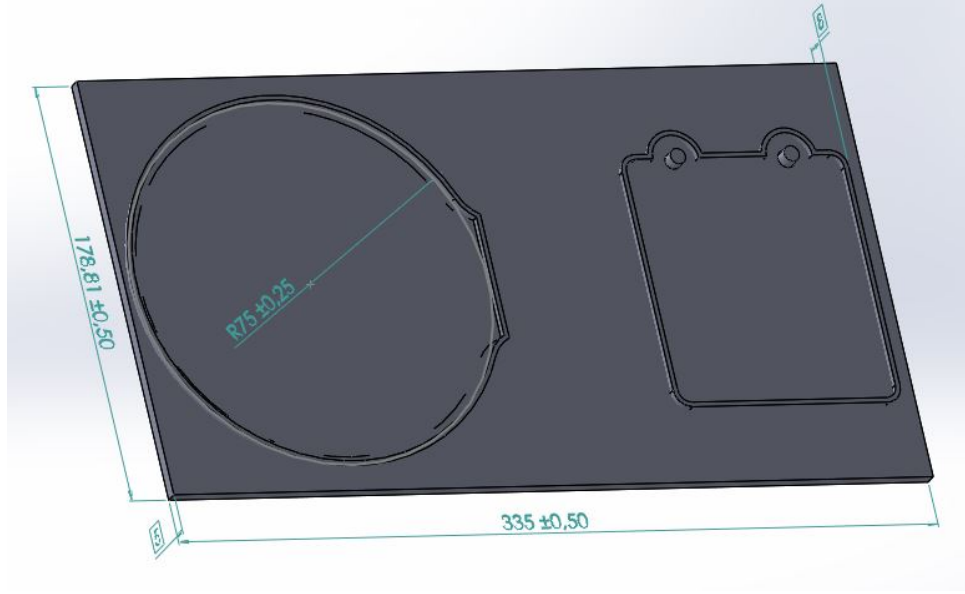


Figure 13: Design of the base

the Mid-Range Transmitter and the haptic device. Thus, only a registration between the environment perceived by the EMTS and the haptic space is needed during the developing of the system.

For this aim, the position of a set of random points is recorded both in the reference system of the EMTS and the haptic device. Then, through linear regression with off-set, the displacement of the origin of the first is computed respect the latter. The obtained equations are the following:

$$\begin{cases} x_{as} = -0.06x_v + 32.36 \\ y_{as} = -0.06y_v - 7.80 \\ z_{as} = -0.03z_v + 20.07 \end{cases} \quad (2.1)$$

In Figure 14, the obtained linear regression lines are shown respect the cloud of recorded

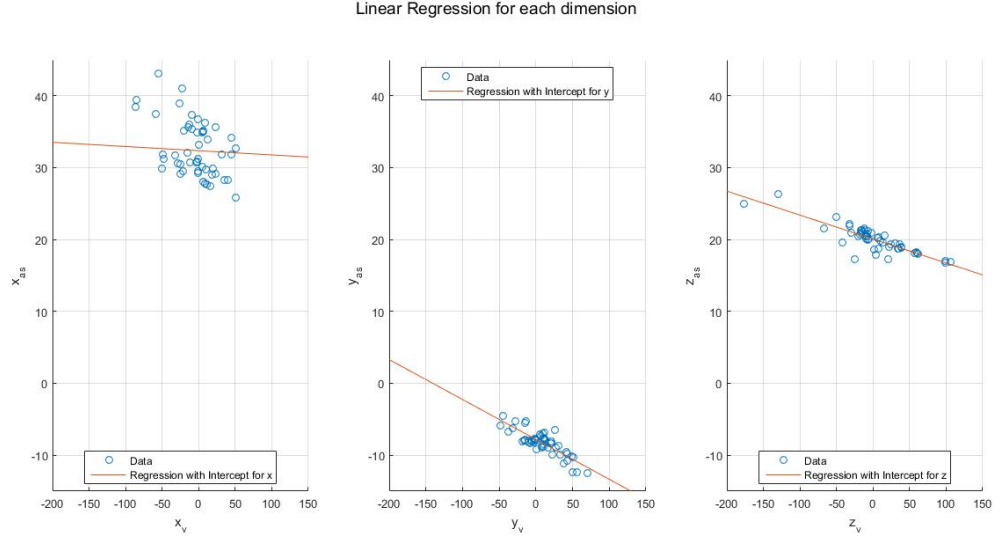


Figure 14: Plot of the obtained regression lines

points. Each subplot represent how the considered coordinate is linearly converted from the tracked values to the virtual environment ones.

The coefficient of determination  $R^2$  measures how well the model can estimate values. It is defined as follows:

$$R^2 = 1 - \frac{\sum_n^1 (x_{as} - \hat{x}_{as})^2}{\sum_n^1 (x_{as} - \bar{x}_{as})^2} \quad (2.2)$$

Where  $\hat{x}_{as}$  represents the calculated values of  $x_{as}$  and  $\bar{x}_{as}$  the mean of the values.

Higher the resulting value is (limit at 1), the better is the model in predicting data. The overall

value is about 0.6, limitations derives from noise due to the closeness of the devices.

In fact, the setting on the base is designed taking qualitatively into account the relative position and feasible distances with less noise, using *CUBES* application by Ascension Technology Corporation. *CUBES* reports in a visual way the quality number, meaning the degree to which the position and angle measurement are imprecise. Generally, errors are caused by the presence of metal in the environment.

Biopsy can be performed with the patient in different positions, e.g. lithotomy position, lateral decubitus or knee-chest[72]. While the registration of the anatomical structures with the virtual environment is computed through the software, the device position is considered in the design phase. The biopsy needle is attached to the stylus of the haptic device aiming the procedure performance helped by the haptic feedback.

Since the needles for PBx are longer than about 16 cm and the workspace in z direction of the haptic device is quite limited also by the its trunk, the haptic device has to be rotated respect the patient. For this project the chosen rotation is of  $90^\circ$  about the vertical axis, also a rotation of  $180^\circ$  about horizontal axis could be used but the fixing in this position and of the base to another support would be troublesome.

### **2.3 Software: LACE Library Description**

*LACE Library* is a C++ software platform acting as a bridge between the operating system and VR applications. It has been implemented at Mixed Reality Lab as development of past projects [73][74][6][54] facing the need to create virtual reality applications incorporating haptic features. It is the result of an integration of four different hardware-software environments:



Figure 15: Hardware setup

- QuickHaptics™ (QH)

It is a MicroAPI built upon Geomagic OpenHaptics®, that is provided for the haptic devices of 3D Systems as a software development toolkit. It is designed to create graphic and haptic application easily, thus used by *LACE Library* for the force rendering.

- Visualization Library (VL)[75]

Based on OpenGL, it is an open-source library combining user-friendliness and intuitiveness with the flexibility and high graphics performances that OpenGL allows.

- Ascension (AS)

Through the C++ 3D Guidance API, the EMTS is integrated into the applications.

- Wykobi Computation Geometry Library (WK)[76]

C++ 2D-3D library used to improve math calculation.

Figure 16 describes how the communication between these libraries is settled in *LACE Library* with the aim to synchronize the several renderings. Information given by the hardware components, like the haptic device, the EMTS and standard input/output hardware (mouse and keyboard) are used by VL to create the graphic rendering and by QH for the tactile and force feedback.

One of the main advantages of *LACE Library* is multithreading, thus the concurrent execution of processes. The haptic thread runs at 1000 Hz to provide a continuous and realistic force feedback and guarantee interaction stability, while optimal results are given by graphic thread at much lower frame rates (60 Hz)[77].

*LACE Library* uses classes to achieve the communication along the four composing libraries. In every application a singleton class, called *LACE Class*, is always created because it stores pointers to the whole set of classes used by the programmer. Its importance resides in the creations, initializations and updates of the various elements present in the application.

The other classes can be grouped in four categories:

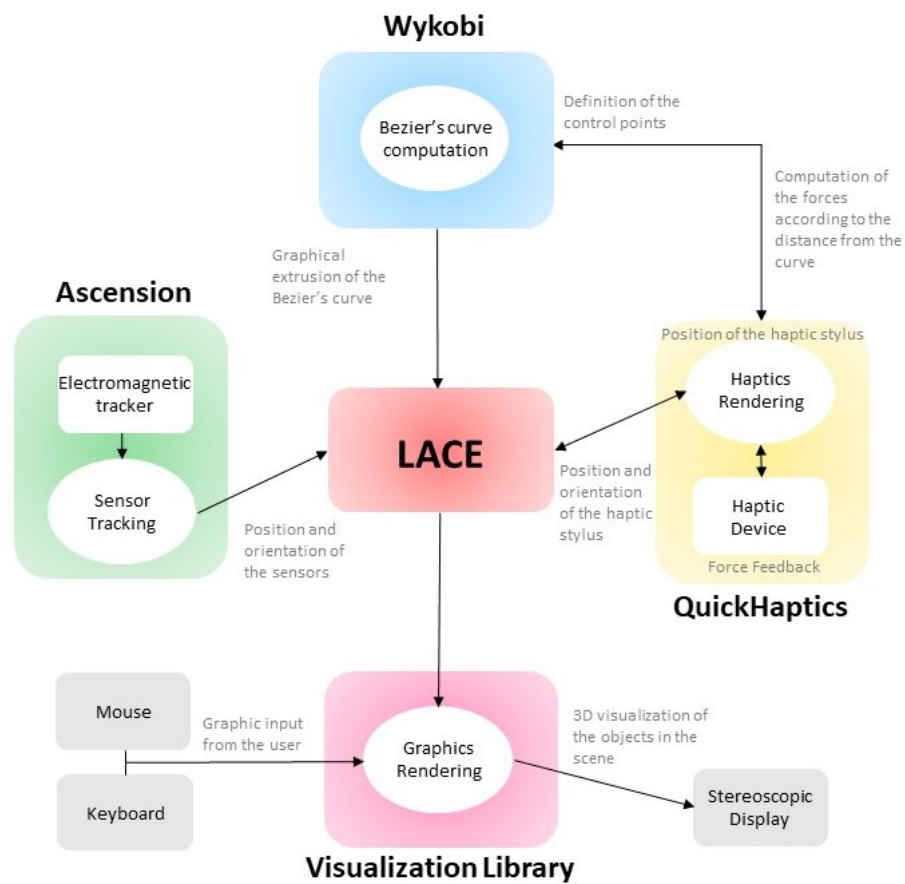


Figure 16: LACE Library Communication Workflow

- Tracking system classes

Classes establishing the communication with AS.

- Renderable Object Classes

This group implement the link between QH and VL. Thus, it is in charge of the creation of object, both simple and complex geometries, that are haptically and graphically rendered.

- Special Forces Classes

One of them is the *LACE Volume Force*, associated to *LACE Volume*, and it allows particular force fields.

- Rendering Classes

*LACE Library* tolerates the definition of multiple renderings in the scene, in this class parameters required for the graphic display are contained.

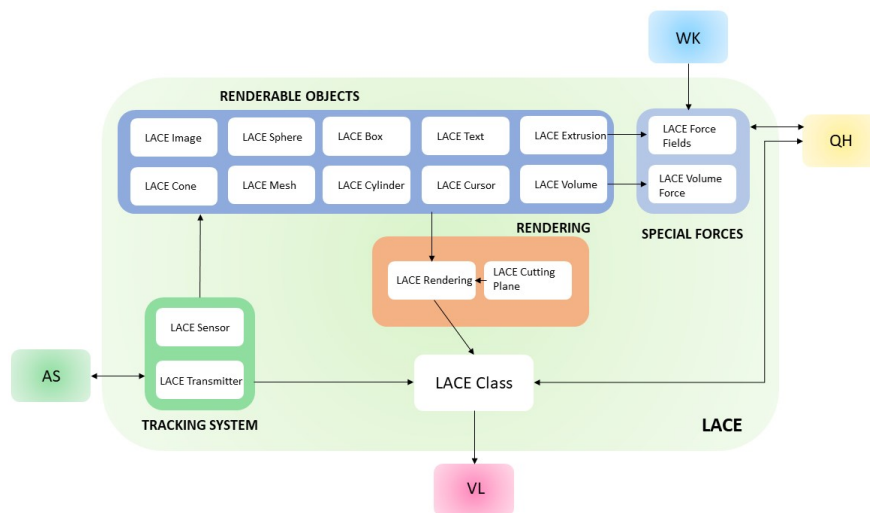


Figure 17: LACE Classes communication

## 2.4 MRI, MRE and Histopathological Datasets Description

The datasets used in the application are composed of 3 pre-operative MRI, 3 ex-vivo MRE and 3 histopathological images, given from [54][78].

### *MRI*

Pelvis MRI is previously obtained respect to radical prostatectomy. The examination was performed on the 3T GE magnet using a phased-array cardiac surface coil providing the following sequences: axial T1 and T2, sagittal and coronal T2, and axial DWI.

From these DICOM images, volume is reconstructed through Volview in MHD format. Volview is an open-source program developed by Kitware, Inc (Clifton Park)[79]. It is intuitive and it allows quick exploration and analysis of 3D medical data.

The resulting volumes have a good spatial resolution on xy plane (512x512), but presenting only 15 sliced on z axis. To provide for this lack of information that results in low accuracy of the registration process, interpolation has been performed. This means that, between two consecutive slices, 15 artificial slices are added, resulting from the weighted mean of the original two slices. From the whole volume, the ROI centered in the prostate gland and with visible fiducial markers is extracted. Then another processing step is computed to reduce the dimensions of the loaded volumes. A manual cast of the voxel values is implemented in order to avoid resolution loss: the conversion is made to obtain eight-bit unsigned char format ranging from 0 to 255. This procedure is just a scale of values into a different range, while characteristics remain unchanged.

### *MRE*

MRE images are acquired through ultra-high-field 9.4T at 500Hz, aiming to detect the wave field displacement along all directions. The obtained slice thickness is of 1mm.

### *Histopathology*

Through radical prostatectomy, the resected organ could be analyzed for histopathologic diagnosis[80]. It is the microscopic study of diseased tissues and a relevant investigative tool. Histopathology is basically the examination of thin tissue sections under microscope, allowing visualization of cells and tissue and recognition of changes due to diseases.

This examination consents the comparison between altered tissue with a control one, with the need of a standardized procedure.

The histopathologic images are obtained increasing stiffness of the prostate though injection of 20cc of 10% buffered formalin. This shrewdness allows thinner slices ( $\sim 3$  mm), thus more consistent.

For prostate histopathology a grossing process is performed removing seminal vesicles, base and apex. It is followed by staining to maintain anatomical orientation. After slicing from apex to base, specimens are quartered and underwent to further processing. Examination to assess PCa is performed through an automatic digital scanner, which stacks the images and allows magnification up to 20 times[81]. Annotation are provided by the pathologist, who contours malignant lesions with RGB colors representing respectively Gleason scores of 5,3,4.

From these 2D images, volumes are created using MATLAB®[82], because of the computation required. After importing in MATLAB® images and dimensions, from each slice ROI of each color is detected and filled. Slices are rescaled according to the dimensions information provided

and proportionally to the individuated bounding boxes. This results in images coherent respect to their actual size and respect to each other.

The centroid of each slice is obtained after binarization of the images and it is used to stack all the slices, recreating a volume.

Arbitrary values are given to the areas superimposed with the ROI indicating lesions, with increasing value according to Gleason score. Due to the low number of slices along z direction, interpolation is required.

## 2.5 Implementation

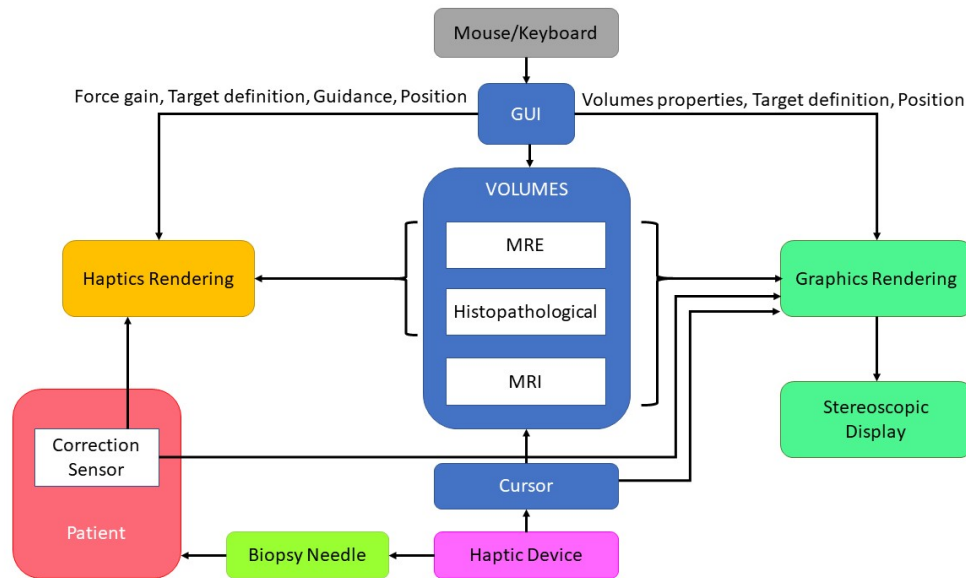


Figure 18: Overview of the application

In Figure 18, an overview of the basic elements that interact in the developed application is shown. The user can manually set parameters related both to the graphics rendering and to the haptics one and to switch between the different modalities and steps.

Next sections explain in detail how the coherence between the two renderings and the real environment is achieved and how the application is developed.

### 2.5.1 Reference System

As mentioned in section 4.3, the haptic device is rotated of  $90^\circ$  about y axis respect its normal usage. This means that what is visualized in the 3D Monitor frontally respect the user has to be perceived laterally respect the body of the haptic device. To achieve coherence between objects graphically and haptically felt, since the reference systems of these environment are turned of  $90^\circ$  one respect the other, the rotation of touchable shapes has to be performed. Analogously, the cursor detected through QH has to be decoupled from the visualized one in order to have consistency. Thus, the displayed needle is a *LACE Mesh* which moves like the cursor but rotated. A mesh is a set of faces, vertices and edges that identify a polyhedral object in computer graphics.

In Figure 19, the interface of *haptic surgical guidance for prostate biopsy* is shown.

### 2.5.2 Volumes Representation

In the virtual environment, volumes from MRI, MRE and histopathology are displayed and loaded in the application in form of *LACE Volumes*. Through this class, VL is exploited thus allowing the visualization of volumes in the following three different modalities:

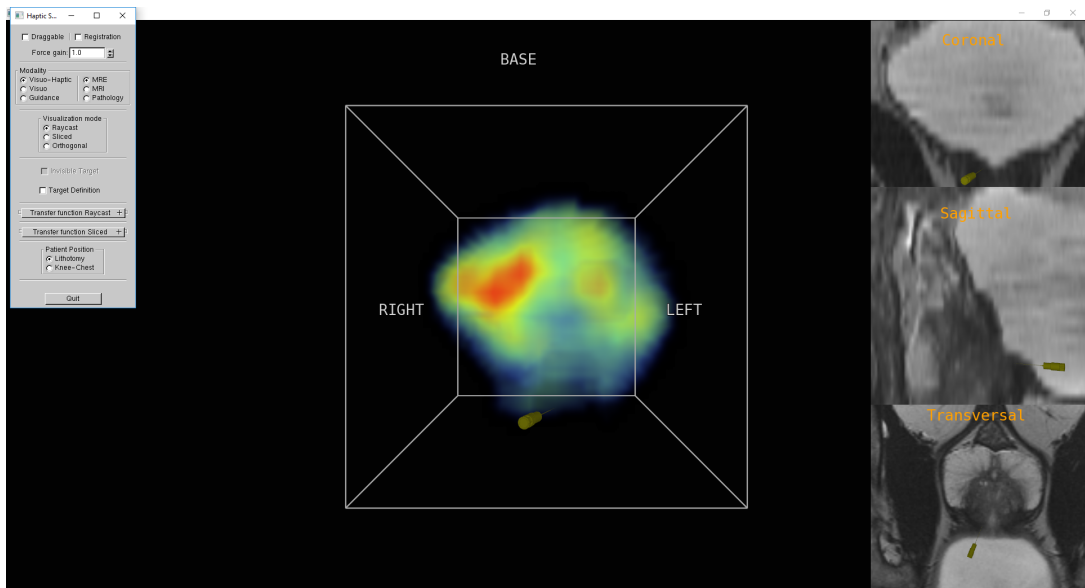


Figure 19: Application Interface

- Volume Raycast

The ray cast technique is used to visualize three-dimensional data. It is based on the 2D projections of a semitransparent volume, thus shooting a ray and sampling along it. For this aim, predefined algorithms can be used, otherwise user-defined algorithms can be loaded. Moreover, R, G, B and  $\alpha$  channels of a custom-made transfer function can be controlled by the user. This kind of visualization is chosen to be the default one because it allows to see internal parts of the volume.

- Volume Sliced

Slices are obtained from the volumetric data and reassembled to obtain the 3D image. The number of slices and RGB transfer function can be defined by the programmer. In

the *haptic surgical guidance for prostate biopsy*, the user can only control the  $\alpha$  value.

Only Volume Sliced can support the *LACE CuttingPlane*, which enable the user to clip the volume through a plane that is originated with location and orientation of the cursor.

- Volume Orthogonal

This modality displays the volume with three bi-dimensional views on the sagittal, axial and coronal planes. Each view depends on the 3D coordinates of the intersection point between all the planes, linking this point to a master-object, like the cursors, will allow the user to control the shown slice.

Bounding box with texts surrounds the prostate in MRE and histopathology volumes for spatial reference especially while interacting with the models. In fact, pressing the first button of the haptic device, the volume is dragged into the virtual environment according to the cursor motion for a better exploration.

While the 3D image is displayed centrally respect the scene created in the application, laterally the 2D orthogonal projections of the MRI volume are shown.

### 2.5.3 Correction Sensor

The volumes position and orientation are tuned by the transformation matrix resulting from a *correction sensor*, if present. It tracks intra-operative displacement of the pelvis. The position of the sensor has to be calibrated respect the position of the haptic device, using offset values from the regression lines (Equation 2.1). *LACE Sensor* and *LACE Transmitter* are used at this stage to obtain respectively the physical communication with the sensor, acquiring the

transform as a quaternion and converting it into a 4x4 matrix, and to control the ON/OFF status of the transmitter.

#### **2.5.4 Registration**

With the aim of consistency of the represented volumes with reality, a registration function is necessary to compute the transformation matrix of the anatomical volume respect the virtual environment. Hence, fiducial markers with coordinates known in both coordinate systems are used, e.g. iliac crests, posterior superior iliac spine, or other anatomical reachable points. During the acquisition of MRI, the patient is scanned with these markers, then these points are touched with the capped needle and memorized. The user can select the patient position between lithotomy and knee-chest to coherently visualize the volumes and markers.

In Figure 20, this registration phase is shown: the orange point is the point which coordinates has to be acquired pressing the first button of the haptic device, green points represent the already obtained coordinates while blue points represent coordinates not acquired yet.

A rigid registration is then performed between the two sets of points. A paired point registration algorithm is used computing the centroids from coordinates, the covariance is calculated, then the obtained covariance matrix is decomposed through Singular Value Decomposition allowing the computation of rotation matrix. The translation is given by the difference of the virtual centroid respect the rotated centroid of anatomical coordinates. To compute the matrix calculations for the Singular Value Decomposition, Eigen library is added[83].

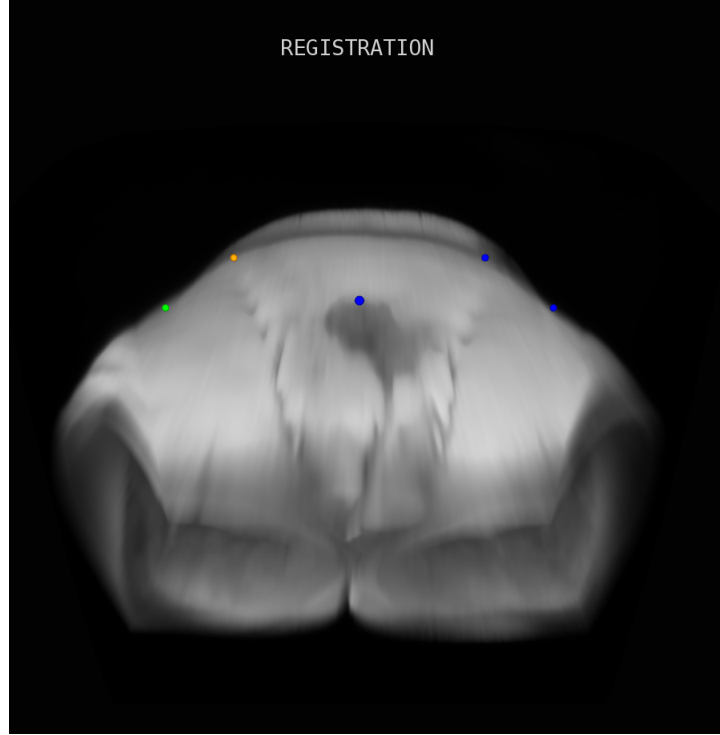


Figure 20: Graphic User Interface

### 2.5.5 Haptic Rendering on Volumes

Haptic rendering is provided while touching volumes with the haptic device. The aim is not to have a realistic feedback, but to enhance the tactile experience for an easily tumor detection. The force that the haptic device returns to the user is based on the stiffness values of both the cursor tip and the surrounding voxels. It is the sum of the force components resulting from elasticity, friction, damping and gravity (compensation):

$$F_{Tot}(x_{Cursor}) = F_{Gravity} + F_{Friction} + F_{Elasticity} + F_{Damping} \quad (2.3)$$

Firstly, the position and direction of motion of the cursor are obtained, then the haptic feedback is given if the cursor is inside the bounding box surrounding the volume and the voxel value touched by the cursor is greater than a threshold.

While the direction is defined accordingly to the cursor motion, the absolute value of the elasticity force is obtained as:

$$|F_{Elasticity}(x_{Cursor})| = (F_{Stiffness} + F_{Gradient}) * gain \quad (2.4)$$

Where the first force component is based on the maximal value of the stiffness of the specific point, while the second term considers the neighboring voxels determining how the values changes in a certain direction. Gain could be modified by the user during the application.

Friction and damping force components are obtained through thresholds.

To avoid unstable feedback and vibrations, the average with the current force and the previous five frames is computed. Furthermore, the resulting value is checked respect the haptic device limits.

### 2.5.6 Haptic Guidance

After the registration procedure, the biopsy can be performed coherently respect the anatomical information. The guidance function provides the user a haptic constrain towards the tumors, assisting him in the core extraction.

Tumors are identified in the MRE images through clustering techniques. This because cluster analysis consists in data organization into representative groups based on similar characteristics.

MRE voxels contain information about the stiffness which ranges from 0 to 255, finding values above an arbitrary threshold (180) leads to the computation of 3D point clouds identifying the tumors.

Subsequently the tumors recognition, the centroid is calculated. It provides a general measure of the cluster location, i.e. the center of mass. The centroid of each cluster is considered as the center of the studied tumor. As first evaluation of this detection technique, the voxels of the histopathologic volume belonging to the range identified by the core dimensions of the needle are considered and found to be higher than the tumor threshold, arbitrarily defined while creating the volume, in almost 90% of cases.

The force guiding the user towards the tumor is a line effect from the insertion point to one tumor at a time implemented in the following way:

1. Detection of the haptic cursor position at the insertion point  $p_i$ , captured when the user presses the first button of the device.
2. Creation of the line from the insertion point to the tumor  $p_t$ .
3. Computation of the wanted haptic position as the projection of the current one on the line.
4. Estimation of force components as the difference between the current position and the desired one, multiplied by an arbitrary gain.
5. Check the upper limit of the force absolute value.

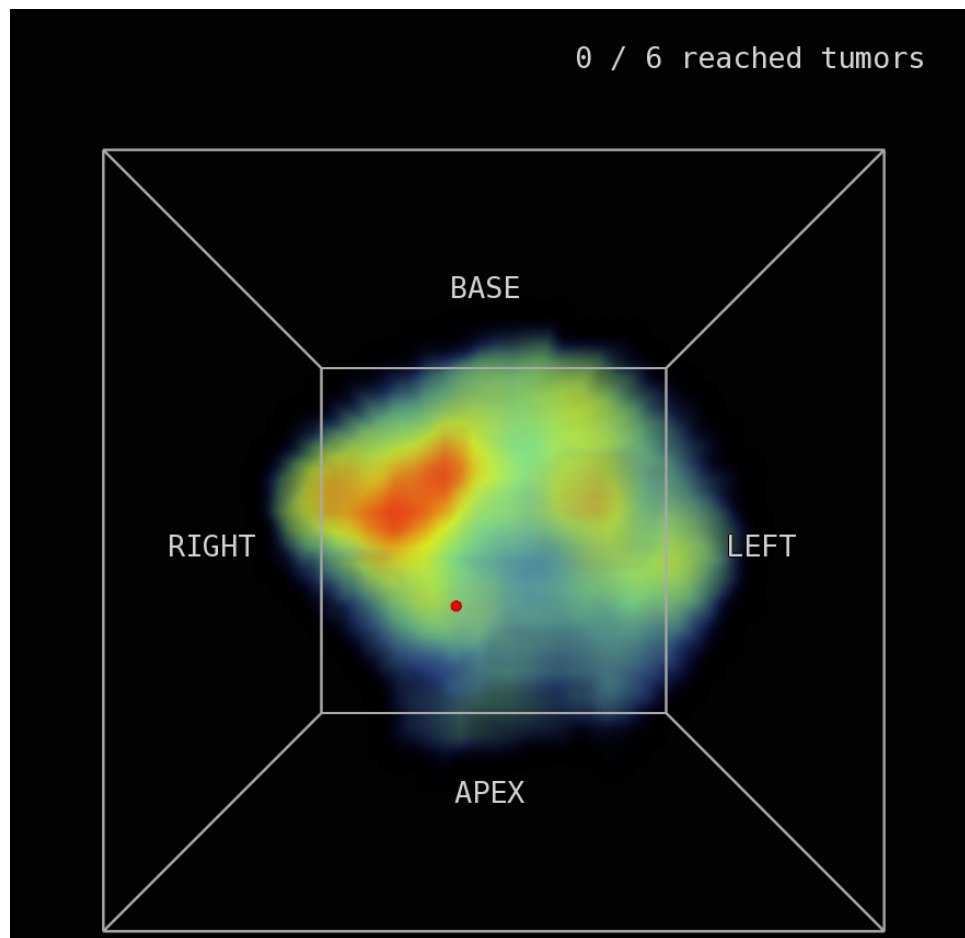


Figure 21: Line Effect

6. Obtain the new force to be applied summing the forces already sent to the device and the computed force.
7. Check if the new force is lower than the half of the physical limits of the haptic device.
8. Address the new force to the haptic device.

The tumor position is automatically updated once the previous tumor is reached with the needle. Moreover, these targets are set to be magnetic, in order to provide a more attractive force towards them.

Furthermore, it has been proved that without visual targets, the user tends to behave with more explorative movements. For this reason, the target is by default visible and can be set invisible according to clinician preferences.

Since the haptic rendering of the volumes could conflict with the line effect, during the guidance process only the latter is present.

During the application, the user can define targets (Figure 22) while the ones obtained through the clustering are shown. The maximum number of user-defined points is given by the difference between an arbitrary maximum number of targets, set to 10, and the identified tumors. Through this function, samples from areas considered suspected by the urologist can be extracted with the haptic guidance. The distance respect the ideal trajectory and the time required to perform the procedure are saved at the end of the process.

### **2.5.7 Graphical User Interface**

The graphical user interface (GUI) is a sub-window through which parameters and modalities are controlled. *LACE Library* relies on GLUI[84], a GLUT based C++ library for the interaction with the user.

GUI, shown in Figure 23, handles the following parameters:

- Switch between modalities, rendering mode of the volumes and tune their transfer function;

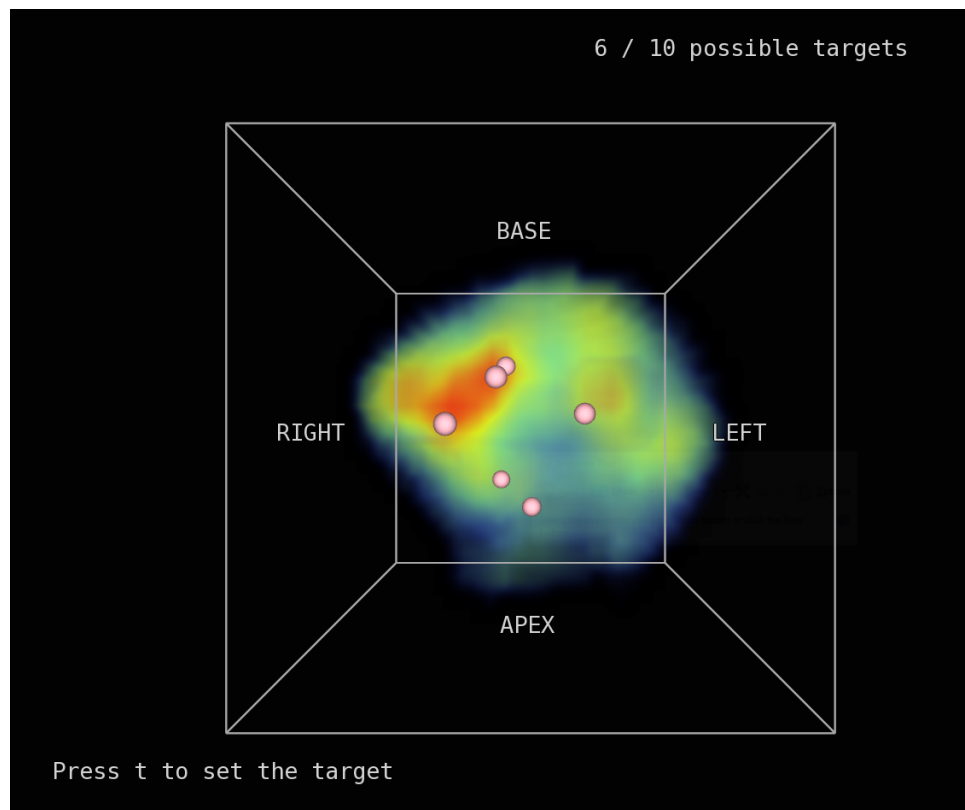


Figure 22: Target Visualization and Definition

- Increase the gain of the haptic feedback;
- Drag the visualized volume;
- Perform the registration;
- Complete biopsy with the guidance.

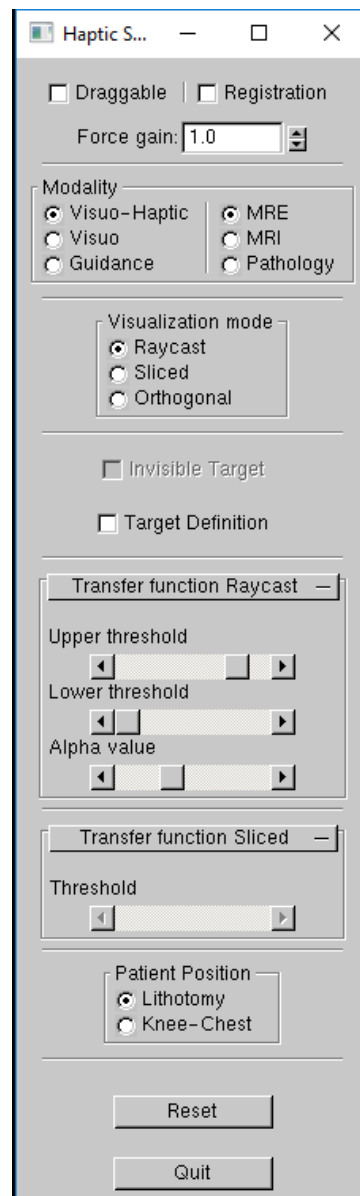


Figure 23: Graphic User Interface

## CHAPTER 3

## CONCLUSION

### 3.1 Discussion and Conclusion

This thesis project aims to develop a tool to perform targeted PBx able to overcome inaccuracy and inefficiency of current procedures.

The proposed solution is a *haptic surgical guidance for prostate biopsy*. The innovation and uniqueness of this approach resides in the targeting of PCa through stiffness parameters obtained with MRE and in the guidance provided towards the center of harder areas with the haptic device.

Concurrently, the 3D graphic interface offers visual and haptic feedback about the prostate gland and the localization of the instrument respect it. The needle position in the operating environment is real-time tracked by the haptic device, thus substituting the TRUS guidance and consequently avoiding deformation of the gland. This is achieved attaching the needle to the stylus of the haptic device.

In order to provide a reliable and valid instrument for pelvis navigation, the virtual environment shows anatomical information given by the three orthogonal projections of the volume and prostate representation with MRE data.

Interaction and exploration of the 3D model of the prostate gland can be conducted with both haptic and visual feedbacks.

The targeting is computed exploiting the stiffness values collected through MRE and the force feedback guides the user towards these points. Moreover, the user can visualize these targets and possibly add other points to reach with the guidance.

This project has been implemented through *LACE Library*, a C++ platform merging four C++ libraries and developed at Mixed Reality Lab as a collateral result of other projects[6][54][73][74]. During the development of this project, general improvements has been brought about it according to the observed problems. Moreover, the considerable usage of *LACE Library* has led debugging. Some classes were designed specifically for certain applications, thus requiring generalization. *LACE Library* is a valid instrument to develop VR applications, allowing efficient communication between the EMTS and graphics rendering, including the real-time haptics rendering.

The *haptic surgical guidance for prostate biopsy* offer a contribute to both bioengineering and urology fields. In particular, it provides a new approach for PBx, which potentially increases accuracy and efficiency.

### **3.2 Future Development**

Firstly, this application has to be validated and assessed. From the Urology Department at University of Illinois at Chicago, students, residents, fellows and faculty will be recruited to test the *haptic surgical guidance for prostate biopsy*. The questionnaire will deal with usefulness, easiness of use, accuracy and safety. In collaboration with Politecnico di Milano, this evaluation phase is planned as continuation of this thesis.

Additional quantitative test of the system to determine its accuracy could be performed.

In particular this project could be improved implementing the target identification in the application instead of using MATLAB®. To avoid the mouse and keyboard, uncomfortable while performing the procedure, a Leap Motion[85] could be introduced to interact with the GUI.

Moreover, further research in MRE is necessary, despite its potential in detecting PCa, there still are some limitations. Firstly, the usefulness of this implemented application is achieved using in-vivo MRE images. This technique has been mainly applied to ex-vivo prostates, while in-vivo studies has only recently begun to be conducted trying to obtain good resolution through the shear waves induction in a patient-friendly method.

A possible extension of this project is to integrate other imaging modalities, like Chemical Exchange Saturation Transfer MRI which permits the visualization of certain compounds, e.g. proteins, with too low concentrations for standard MRI.

## APPENDICES

## Appendix A

### B-SPLINE REGISTRATION

The goal is to relate any point of one image to the reference one [64], meaning to find the optimal transformation  $T:(x, y, z) \mapsto (x', y', z')$ . To take into account the deformation, the transformation  $T$  is given by global and local transformations:

$$T(x, y, z) = T_{Global}(x, y, z) + T_{Local}(x, y, z) \quad (\text{A.1})$$

The global motion model can be described in the easier approach as a rigid transformation with six degrees of freedom, thus using an affine transformation.

$$T(x, y, z) = T_{Global}(x, y, z) + T_{Local}(x, y, z) \quad (\text{A.2})$$

The global motion model can be described in the easier approach as a rigid transformation with six degrees of freedom, thus using an affine transformation.

$$T_{Global}(x, y, z) = \begin{pmatrix} \theta_{11} & \theta_{12} & \theta_{13} \\ \theta_{21} & \theta_{22} & \theta_{23} \\ \theta_{31} & \theta_{32} & \theta_{33} \end{pmatrix} \begin{pmatrix} x \\ y \\ z \end{pmatrix} + \begin{pmatrix} \theta_{14} \\ \theta_{24} \\ \theta_{34} \end{pmatrix} \quad (\text{A.3})$$

## Appendix A (continued)

To model the local deformation an additional transformation matrix is required. A powerful tool to model 3D deformable objects is the free-form deformation model based on B-splines. The idea is that the deformation is computed creating a mesh  $(n_x \times n_y \times n_z)$  of control points uniformly spaced. Thus,

$$T_{Local}(x, y, z) = \sum_{l=0}^3 \sum_{m=0}^3 \sum_{n=0}^3 B_l(u) B_m(v) B_n(w) \phi_{i+l, j+m, k+n} \quad (\text{A.4})$$

where  $i = x/n_x - 1, j = y/n_y - 1, k = z/n_z - 1, u = x/n_x - \lfloor x/n_x \rfloor, v = y/n_y - \lfloor y/n_y \rfloor, z = z/n_z - \lfloor z/n_z \rfloor$  and  $B_j$  represents the  $j^{th}$  B-spline basis function:

$$B_0(u) = (1-u)^3/6; B_1(u) = (3u^3 - 6u^2 + 4)/6; B_2(u) = (-3u^3 + 3u^2 + 3u + 1)/6; B_3(u) = u^3/6. \quad (\text{A.5})$$

Generally, the local tissue deformation is characterized by smooth transition, to consider this aspect in the computation a penalty term is added:

$$C_{smooth} = \frac{1}{V} \int_0^X \int_0^Y \int_0^Z \left[ \left( \frac{\partial^2 T}{\partial x^2} \right)^2 + \left( \frac{\partial^2 T}{\partial y^2} \right)^2 + \left( \frac{\partial^2 T}{\partial z^2} \right)^2 + 2 \left( \frac{\partial^2 T}{\partial xy} \right)^2 + 2 \left( \frac{\partial^2 T}{\partial xz} \right)^2 + 2 \left( \frac{\partial^2 T}{\partial yz} \right)^2 \right] dx dy dz \quad (\text{A.6})$$

where V represents the volume of the image domain. Through a similarity criterion, the degree of alignment of two images (A and B) is measured using their entropy:

$$C_{similarity}(A, B) = \frac{H(A) + H(B)}{H(A, B)}. \quad (\text{A.7})$$

## Appendix A (continued)

The optimal transformation is finally obtained minimizing the cost function associated to the global ( $\theta$ ) and local ( $\phi$ ) transforms:




$$C(\theta, \phi) = -C_{similarity}(I(t_0), T(I(t))) + \lambda C_{smooth}(T), \quad (\text{A.8})$$


being  $\lambda$  a weighting parameter.



## Appendix B


### FIGURES PERMISSION

Permission request for prostate images Inbox x

**Martina Berni** <mberni3@uic.edu>


Apr 11 (8 days ago) ★  


to Katja 



Dear Kathleen Tetzlaff,


I am a bioengineering Master's student writing my master thesis with professor Luciano dealing with prostate cancer. I have seen the images that you gave to Lorenzo Rapetti and Eleonora Tagliabue for their thesis and I would like to ask you the permission to use them also for my work.

Thank you,  
Martina



**Tetzlaff, Katja**

Apr 12 (7 days ago) ★  

to me 

Hi Martina,

Thanks for messaging me. The images you are referring to were created for the thesis work of David Zumba. I was unaware that other MS/PhD students such as Lorenzo Rapetti and Eleonora Tagliabue were also using these images, as no one contacted me for permission. I don't mind you or these other students using my images but I do require that I receive notification before they are used and that they are properly cited/I receive credit for my work, particularly since these images were created without any monetary compensation.

I will follow-up with Professor Luciano so he can be aware of the stipulations on using my work.

Please let me know if you have additional questions.

Thank you,  
Katja

## Appendix B (continued)

1/5/2018

RightsLink Printable License

### SPRINGER NATURE LICENSE TERMS AND CONDITIONS

May 01, 2018

This Agreement between University of Illinois at Chicago ("You") and Springer Nature ("Springer Nature") consists of your license details and the terms and conditions provided by Springer Nature and Copyright Clearance Center.

License Number	4340340091738
License date	May 01, 2018
Licensed Content Publisher	Springer Nature
Licensed Content Publication	Abdominal Imaging
Licensed Content Title	Magnetic resonance elastography of abdomen
Licensed Content Author	Sudhakar Kundapur Venkatesh, Richard L. Ehman
Licensed Content Date	Jan 1, 2014
Licensed Content Volume	40
Licensed Content Issue	4
Type of Use	Thesis/Dissertation
Requestor type	academic/university or research institute
Format	print and electronic
Portion	figures/tables/illustrations
Number of figures/tables/illustrations	2
Will you be translating?	no
Circulation/distribution	<501
Author of this Springer Nature content	no
Title	Haptic Surgical Guidance for Prostate Biopsy
Instructor name	Cristian Luciano
Institution name	University of Illinois at Chicago
Expected presentation date	May 2018
Portions	Figure 2
Requestor Location	University of Illinois at Chicago 1910 N Mozart St  CHICAGO, IL 60647 United States Attn: University of Illinois at Chicago
Billing Type	Invoice
Billing Address	University of Illinois at Chicago 1910 N Mozart St  CHICAGO, IL 60647 United States Attn: University of Illinois at Chicago
Total	0.00 USD
Terms and Conditions	

## Appendix B (continued)

1/5/2018

RightsLink Printable License

### Springer Nature Terms and Conditions for RightsLink Permissions

**Springer Customer Service Centre GmbH (the Licensor)** hereby grants you a non-exclusive, world-wide licence to reproduce the material and for the purpose and requirements specified in the attached copy of your order form, and for no other use, subject to the conditions below:

1. The Licensor warrants that it has, to the best of its knowledge, the rights to license reuse of this material. However, you should ensure that the material you are requesting is original to the Licensor and does not carry the copyright of another entity (as credited in the published version).

If the credit line on any part of the material you have requested indicates that it was reprinted or adapted with permission from another source, then you should also seek permission from that source to reuse the material.

2. Where **print only** permission has been granted for a fee, separate permission must be obtained for any additional electronic re-use.
3. Permission granted **free of charge** for material in print is also usually granted for any electronic version of that work, provided that the material is incidental to your work as a whole and that the electronic version is essentially equivalent to, or substitutes for, the print version.
4. A licence for 'post on a website' is valid for 12 months from the licence date. This licence does not cover use of full text articles on websites.
5. Where '**reuse in a dissertation/thesis**' has been selected the following terms apply: Print rights for up to 100 copies, electronic rights for use only on a personal website or institutional repository as defined by the Sherpa guideline ([www.sherpa.ac.uk/romeo/](http://www.sherpa.ac.uk/romeo/)).
6. Permission granted for books and journals is granted for the lifetime of the first edition and does not apply to second and subsequent editions (except where the first edition permission was granted free of charge or for signatories to the STM Permissions Guidelines <http://www.stm-assoc.org/copyright-legal-affairs/permissions/permissions-guidelines/>), and does not apply for editions in other languages unless additional translation rights have been granted separately in the licence.
7. Rights for additional components such as custom editions and derivatives require additional permission and may be subject to an additional fee. Please apply to [Journalpermissions@springernature.com](mailto:Journalpermissions@springernature.com)/[bookpermissions@springernature.com](mailto:bookpermissions@springernature.com) for these rights.
8. The Licensor's permission must be acknowledged next to the licensed material in print. In electronic form, this acknowledgement must be visible at the same time as the figures/tables/illustrations or abstract, and must be hyperlinked to the journal/book's homepage. Our required acknowledgement format is in the Appendix below.
9. Use of the material for incidental promotional use, minor editing privileges (this does not include cropping, adapting, omitting material or any other changes that affect the meaning, intention or moral rights of the author) and copies for the disabled are permitted under this licence.
10. Minor adaptations of single figures (changes of format, colour and style) do not require the Licensor's approval. However, the adaptation should be credited as shown in Appendix below.

### Appendix — Acknowledgements:

#### **For Journal Content:**

Reprinted by permission from [the Licensor]: [Journal Publisher (e.g. Nature/Springer/Palgrave)] [JOURNAL NAME] [REFERENCE CITATION (Article name, Author(s) Name), [COPYRIGHT] (year of publication)]

#### **For Advance Online Publication papers:**

Reprinted by permission from [the Licensor]: [Journal Publisher (e.g.

## Appendix B (continued)

1/5/2018

RightsLink Printable License

Nature/Springer/Palgrave)] [JOURNAL NAME] [REFERENCE CITATION  
(Article name, Author(s) Name), [COPYRIGHT] (year of publication), advance  
online publication, day month year (doi: 10.1038/sj.[JOURNAL ACRONYM].)

### For Adaptations/Translations:

Adapted/Translated by permission from [the Licensor]: [Journal Publisher (e.g.  
Nature/Springer/Palgrave)] [JOURNAL NAME] [REFERENCE CITATION  
(Article name, Author(s) Name), [COPYRIGHT] (year of publication)

### **Note: For any republication from the British Journal of Cancer, the following credit line style applies:**

Reprinted/adapted/translated by permission from [the Licensor]: on behalf of Cancer  
Research UK: : [Journal Publisher (e.g. Nature/Springer/Palgrave)] [JOURNAL  
NAME] [REFERENCE CITATION (Article name, Author(s) Name),  
[COPYRIGHT] (year of publication)

### For Advance Online Publication papers:

Reprinted by permission from The [the Licensor]: on behalf of Cancer Research UK:  
[Journal Publisher (e.g. Nature/Springer/Palgrave)] [JOURNAL NAME]  
[REFERENCE CITATION (Article name, Author(s) Name), [COPYRIGHT] (year  
of publication), advance online publication, day month year (doi: 10.1038/sj.  
[JOURNAL ACRONYM])

### For Book content:

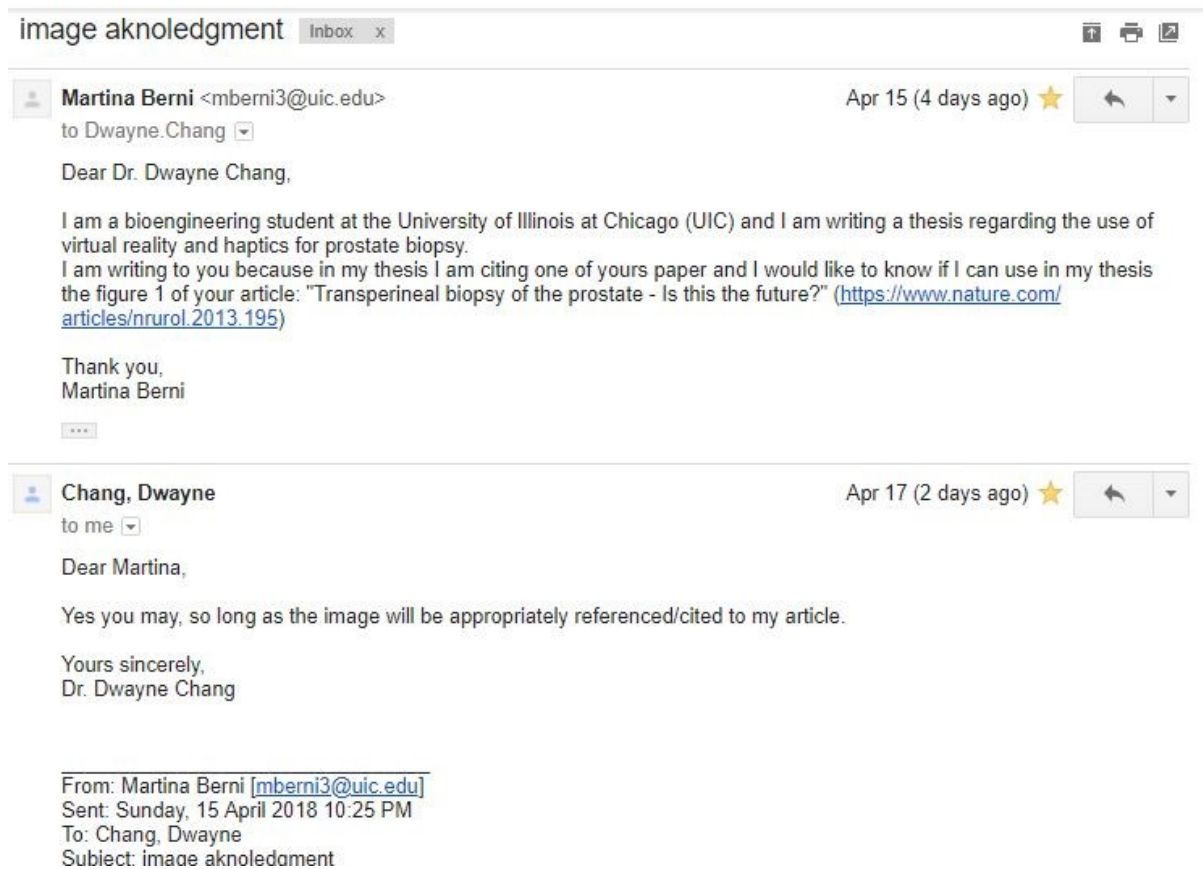
Reprinted/adapted by permission from [the Licensor]: [Book Publisher (e.g.  
Palgrave Macmillan, Springer etc) [Book Title] by [Book author(s)]  
[COPYRIGHT] (year of publication)

### Other Conditions:

Version 1.0

Questions? [customercare@copyright.com](mailto:customercare@copyright.com) or +1-855-239-3415 (toll free in the US) or  
+1-978-646-2777.

## Appendix B (continued)



## CITED LITERATURE

1. American cancer society. <https://www.cancer.org/cancer/prostate-cancer/about/key-statistics.html>. Accessed: 2018-03-28.
2. Sosnowski, R., Zagrodzka, M., and Borkowski, T.: The limitations of multiparametric magnetic resonance imaging also must be borne in mind. Central European journal of urology, 69(1):22, 2016.
3. Turkbey, B., Pinto, P. A., Mani, H., Bernardo, M., Pang, Y., McKinney, Y. L., Khurana, K., Ravizzini, G. C., Albert, P. S., Merino, M. J., et al.: Prostate cancer: value of multiparametric mr imaging at 3 t for detectionhistopathologic correlation. Radiology, 255(1):89–99, 2010.
4. van de Ven, W. J., Sedelaar, J. M., van der Leest, M. M., Hulsbergen-van de Kaa, C. A., Barentsz, J. O., Fütterer, J. J., and Huisman, H. J.: Visibility of prostate cancer on transrectal ultrasound during fusion with multiparametric magnetic resonance imaging for biopsy. Clinical imaging, 40(4):745–750, 2016.
5. Marks, L., Young, S., and Natarajan, S.: Mri-ultrasound fusion for guidance of targeted prostate biopsy. Current opinion in urology, 23(1):43, 2013.
6. Rapetti, L.: Virtual reality navigation system for prostate biopsy, 2017.
7. National cancer institute. <https://training.seer.cancer.gov/prostate/anatomy/>. Accessed: 2018-03-28.
8. Canadian cancer society. <http://www.cancer.ca/en/cancer-information/cancer-type/prostate/prostate-cancer/the-prostate/?region=on>. Accessed: 2018-03-28.
9. Medscape. <https://emedicine.medscape.com/article/1923122-overview#a2>. Accessed: 2018-03-28.
10. Innerbody. [http://www.innerbody.com/image\\_repmov/repo09-new4.html](http://www.innerbody.com/image_repmov/repo09-new4.html). Accessed: 2018-03-28.

### CITED LITERATURE (continued)

11. Pubmed health. <https://www.ncbi.nlm.nih.gov/pubmedhealth/PMH0072475/>. Accessed: 2018-03-28.
12. Sperling prostate center. <https://sperlingprostatecenter.com/prostate-zone-anatomy-prostate-cancer-and-imaging/>. Accessed: 2018-03-28.
13. Life science. <https://www.livescience.com/32751-what-does-the-prostate-gland-do.html>. Accessed: 2018-03-28.
14. Andreoiu, M. and Cheng, L.: Multifocal prostate cancer: biologic, prognostic, and therapeutic implications. Human pathology, 41(6):781–793, 2010.
15. National cancer institute. <https://www.cancer.gov/types/prostate/psa-fact-sheet>. Accessed: 2018-03-28.
16. Hoffman: Screening for prostate cancer. The New England Journal of Medicine, 1(365):2013–2019, 2011.
17. Bjurlin, M. A., Mendhiratta, N., Wysock, J. S., and Taneja, S. S.: Multiparametric mri and targeted prostate biopsy: improvements in cancer detection, localization, and risk assessment. Central European journal of urology, 69(1):9, 2016.
18. Ghai, S. and Haider, M. A.: Multiparametric-mri in diagnosis of prostate cancer. Indian journal of urology: IJU: journal of the Urological Society of India, 31(3):194, 2015.
19. Harvey, H. and deSouza, N. M.: The role of imaging in the diagnosis of primary prostate cancer. Journal of clinical urology, 9(2\_suppl):11–17, 2016.
20. Prostate conditions education council. <https://www.prostateconditions.org/about-prostate-conditions/prostate-cancer/newly-diagnosed/gleason-score>. Accessed: 2018-03-28.
21. Jie, C., Rongbo, L., and Ping, T.: The value of diffusion-weighted imaging in the detection of prostate cancer: a meta-analysis. European radiology, 24(8):1929–1941, 2014.
22. Hegde, J. V., Mulkern, R. V., Panych, L. P., Fennessy, F. M., Fedorov, A., Maier, S. E., and Tempany, C.: Multiparametric mri of prostate cancer: An update on state-of-the-art techniques and their performance in detecting and localizing prostate cancer. Journal of magnetic resonance imaging, 37(5):1035–1054, 2013.

### CITED LITERATURE (continued)

23. Fusco, R., Sansone, M., Granata, V., Setola, S. V., and Petrillo, A.: A systematic review on multiparametric mr imaging in prostate cancer detection. Infectious agents and cancer, 12(1):57, 2017.
24. Guo, L.-H., Wu, R., Xu, H.-X., Xu, J.-M., Wu, J., Wang, S., Bo, X.-W., and Liu, B.-J.: Comparison between ultrasound guided transperineal and transrectal prostate biopsy: a prospective, randomized, and controlled trial. Scientific reports, 5:16089, 2015.
25. Chang, D. T., Challacombe, B., and Lawrentschuk, N.: Transperineal biopsy of the prostate is this the future? Nature Reviews Urology, 10(12):690, 2013.
26. Miller, J., Perumalla, C., and Heap, G.: Complications of transrectal versus transperineal prostate biopsy. ANZ journal of surgery, 75(1-2):48–50, 2005.
27. Takenaka, A., Hara, R., Ishimura, T., Fujii, T., Jo, Y., Nagai, A., and Fujisawa, M.: A prospective randomized comparison of diagnostic efficacy between transperineal and transrectal 12-core prostate biopsy. Prostate cancer and prostatic diseases, 11(2):134, 2008.
28. Quon, J. S., Moosavi, B., Khanna, M., Flood, T. A., Lim, C. S., and Schieda, N.: False positive and false negative diagnoses of prostate cancer at multi-parametric prostate mri in active surveillance. Insights into imaging, 6(4):449–463, 2015.
29. Serefoglu, E. C., Altinova, S., Ugras, N. S., Akincioglu, E., Asil, E., and Balbay, M. D.: How reliable is 12-core prostate biopsy procedure in the detection of prostate cancer? Canadian Urological Association Journal, 7(5-6):E293, 2013.
30. Hodge, K. K., McNeal, J. E., Terris, M. K., and Stamey, T. A.: Random systematic versus directed ultrasound guided transrectal core biopsies of the prostate. The Journal of urology, 142(1):71–74, 1989.
31. Djavan, B., Remzi, M., Schulman, C. C., Marberger, M., and Zlotta, A. R.: Repeat prostate biopsy: who, how and when?: a review. European urology, 42(2):93–103, 2002.
32. Brock, M., von Bodman, C., Palisaar, J., Becker, W., Martin-Seidel, P., and Noldus, J.: Detecting prostate cancer: a prospective comparison of systematic prostate biopsy with targeted biopsy guided by fused mri and transrectal ultrasound. Deutsches Ärzteblatt International, 112(37):605, 2015.

### CITED LITERATURE (continued)

33. Bjurlin, M. A., Wysock, J. S., and Taneja, S. S.: Optimization of prostate biopsy: review of technique and complications. Urologic Clinics, 41(2):299–313, 2014.
34. Murphy, I. G., NiMhurchu, E., Gibney, R. G., and McMahon, C. J.: Mri-directed cognitive fusion-guided biopsy of the anterior prostate tumors. Diagnostic and Interventional Radiology, 23(2):87, 2017.
35. Addicott, B., Foster, B. R., Johnson, C., Fung, A., Amling, C. L., and Coakley, F. V.: Direct magnetic resonance imaging-guided biopsy of the prostate: lessons learned in establishing a regional referral center. Translational andrology and urology, 6(3):395, 2017.
36. Kongnyuy, M., George, A. K., Rastinehad, A. R., and Pinto, P. A.: Magnetic resonance imaging-ultrasound fusion-guided prostate biopsy: review of technology, techniques, and outcomes. Current urology reports, 17(4):32, 2016.
37. Figueras-Benítez, G., Urbano, L., Acero, A., Huerta, M., and Castro, M.: Surgical navigation systems: A technological overview. In VII International Conference on Electrical Engineering Surgical navigation systems, Technological overview corregido, 2014.
38. Mezger, U., Jendrewski, C., and Bartels, M.: Navigation in surgery. Langenbeck’s archives of surgery, 398(4):501–514, 2013.
39. Nazir, B.: Pain during transrectal ultrasound-guided prostate biopsy and the role of periprostatic nerve block: what radiologists should know. Korean journal of radiology, 15(5):543–553, 2014.
40. Madej, A., Wilkosz, J., Róžański, W., and Lipiński, M.: Complication rates after prostate biopsy according to the number of sampled cores. Central European journal of urology, 65(3):116, 2012.
41. Webmd. <https://www.webmd.com/prostate-cancer/prostate-cancer-stages#1>. Accessed: 2018-03-28.
42. Litwin, M. S. and Tan, H.-J.: The diagnosis and treatment of prostate cancer: a review. Jama, 317(24):2532–2542, 2017.

### CITED LITERATURE (continued)

43. Kemper, J., Sinkus, R., Lorenzen, J., Nolte-Ernsting, C., Stork, A., and Adam, G.: Mr elastography of the prostate: initial in-vivo application. In RöFo-Fortschritte auf dem Gebiet der Röntgenstrahlen und der bildgebenden Verfahren, volume 176, pages 1094–1099. © Georg Thieme Verlag KG Stuttgart· New York, 2004.
44. Pepin, K. M., Ehman, R. L., and McGee, K. P.: Magnetic resonance elastography (mre) in cancer: Technique, analysis, and applications. Progress in nuclear magnetic resonance spectroscopy, 90:32–48, 2015.
45. Venkatesh, S. K. and Ehman, R. L.: Magnetic resonance elastography of abdomen. Abdominal imaging, 40(4):745–759, 2015.
46. Jackson, B. G. and Rosenberg, L.: Force feedback and medical simulation. Interactive Technology and the New Paradigm for Healthcare, Morgan et al.(Eds), pages 147–151, 1995.
47. Ullrich, S. and Kuhlen, T.: Haptic palpation for medical simulation in virtual environments. IEEE Transactions on Visualization and Computer Graphics, 18(4):617–625, 2012.
48. Basdogan, C., De, S., Kim, J., Muniyandi, M., Kim, H., and Srinivasan, M. A.: Haptics in minimally invasive surgical simulation and training. IEEE computer graphics and applications, 24(2):56–64, 2004.
49. Burdea, G., Patounakis, G., Popescu, V., and Weiss, R. E.: Virtual reality-based training for the diagnosis of prostate cancer. IEEE Transactions on Biomedical engineering, 46(10):1253–1260, 1999.
50. Khaled, W., Reichling, S., Bruhns, O., Boese, H., Baumann, M., Monkman, G., Egersdoerfer, S., Klein, D., Tunayar, A., Freimuth, H., et al.: Palpation imaging using a haptic system for virtual reality applications in medicine. In Perspective In Image-Guided Surgery, pages 407–414. World Scientific, 2004.
51. Palmerius, K. L., Havre, R. F., Gilja, O. H., and Viola, I.: Ultrasound palpation by haptic elastography. In Computer-Based Medical Systems (CBMS), 2011 24th International Symposium on, pages 1–6. IEEE, 2011.
52. Suga, M., Matsuda, T., Minato, K., Oshiro, O., Chihara, K., Okamoto, J., Takizawa, O., Komori, M., and Takahashi, T.: Measurement of in-vivo local shear modulus by combining multiple phase offsets mr elastography. Studies in health technology and informatics, (2):933–937, 2001.

### CITED LITERATURE (continued)

53. Li, B. N., Shan, X., Qin, J., Huang, W., and An, N.: Senseviewer: A unified rendering interface of visual and haptic cues in medical images. In Robotics and Biomimetics (ROBIO), 2013 IEEE International Conference on, pages 2209–2212. IEEE, 2013.
54. Tagliabue, E.: Visuo-haptic model of prostate cancer based on magnetic resonance elastography, 2017.
55. Giganti, F. and Moore, C. M.: A critical comparison of techniques for mri-targeted biopsy of the prostate. Translational andrology and urology, 6(3):432, 2017.
56. Filson, C. P., Natarajan, S., Margolis, D. J., Huang, J., Lieu, P., Dorey, F. J., Reiter, R. E., and Marks, L. S.: Prostate cancer detection with magnetic resonance-ultrasound fusion biopsy: The role of systematic and targeted biopsies. Cancer, 122(6):884–892, 2016.
57. Xu, S., Kruecker, J., Turkbey, B., Glossop, N., Singh, A. K., Choyke, P., Pinto, P., and Wood, B. J.: Real-time mri-trus fusion for guidance of targeted prostate biopsies. Computer Aided Surgery, 13(5):255–264, 2008.
58. Sahebjavaher, R. S., Nir, G., Honarvar, M., Gagnon, L. O., Ischia, J., Jones, E. C., Chang, S. D., Fazli, L., Goldenberg, S. L., Rohling, R., et al.: Mr elastography of prostate cancer: quantitative comparison with histopathology and repeatability of methods. NMR in Biomedicine, 28(1):124–139, 2015.
59. Van der Meijden, O. and Schijven, M.: The value of haptic feedback in conventional and robot-assisted minimal invasive surgery and virtual reality training: a current review. Surgical endoscopy, 23(6):1180–1190, 2009.
60. Avila, R. S. and Sobierajski, L. M.: A haptic interaction method for volume visualization. In Visualization’96. Proceedings., pages 197–204. IEEE, 1996.
61. Griffiths, P. G. and Gillespie, R. B.: Sharing control between humans and automation using haptic interface: primary and secondary task performance benefits. Human factors, 47(3):574–590, 2005.
62. Mugge, W., Kuling, I. A., Brenner, E., and Smeets, J. B.: Haptic guidance needs to be intuitive not just informative to improve human motor accuracy. PloS one, 11(3):e0150912, 2016.

# CITED LITERATURE (continued)

63. Wyawahare, M. V., Patil, P. M., Abhyankar, H. K., et al.: Image registration techniques: an overview. International Journal of Signal Processing, Image Processing and Pattern Recognition, 2(3):11–28, 2009.
64. Rueckert, D., Sonoda, L. I., Hayes, C., Hill, D. L., Leach, M. O., and Hawkes, D. J.: Nonrigid registration using free-form deformations: application to breast mr images. IEEE transactions on medical imaging, 18(8):712–721, 1999.
65. Herlambang, N., Liao, H., Matsumiya, K., Masamune, K., and Dohi, T.: Physically accurate b-spline based non-rigid registration using variable spring model. In Biomedical Imaging: From Nano to Macro, 2007. ISBI 2007. 4th IEEE International Symposium on, pages 748–751. IEEE, 2007.
66. Slicer3d. <https://www.slicer.org/>. Accessed: 2018-04-10.
67. Itk. <https://itk.org/>. Accessed: 2018-04-10.
68. Keszei, A. P., Berkels, B., and Deserno, T. M.: Survey of non-rigid registration tools in medicine. Journal of digital imaging, 30(1):102–116, 2017.
69. 3d systems. <https://www.3dsystems.com/software>. Accessed: 2018-04-10.
70. Ascension technology corporation. <https://www.ascension-tech.com/>. Accessed: 2018-04-10.
71. Soliworks. <https://www.solidworks.com/>. Accessed: 2018-04-10.
72. Lodeta, B. and Lodeta, M.: Prostate biopsy in the left lateral decubitus position is less painful than prostate biopsy in the lithotomy position: a randomized controlled trial. Korean journal of urology, 53(2):87–91, 2012.
73. Faso, A.: Haptic and virtual reality surgical simulator for training in percutaneous renal access, 2017.
74. Gatti, C.: Application of haptic virtual fixtures in psychomotor skill development for robotic surgical training, 2017.
75. Visualization library. <http://visualizationlibrary.org/docs/2.0/html/index.html>. Accessed: 2018-04-10.

# CITED LITERATURE (continued)

76. Wykobi. <http://www.wykobi.com/>. Accessed: 2018-04-10.
77. Magnenat-Thalmann, N. and Bonanni, U.: Haptics in virtual reality and multimedia. IEEE MultiMedia, 13(3):6–11, 2006.
78. Caldwell, B.: Correlating histopathology and radiologic imaging to validate prostate cancer detection, 2018.
79. Volview. <https://www.kitware.com/volview/>. Accessed: 2018-04-10.
80. Slaoui, M. and Fiette, L.: Histopathology procedures: from tissue sampling to histopathological evaluation. In Drug safety Evaluation, pages 69–82. Springer, 2011.
81. Leica, aperio at2. <https://www.leicabiosystems.com/digital-pathology/scan/aperio-at2/>. Accessed: 2018-04-10.
82. Matlab. <https://www.mathworks.com/products/matlab.html>. Accessed: 2018-04-10.
83. Eigen. [http://eigen.tuxfamily.org/index.php?title=Main\\_Page](http://eigen.tuxfamily.org/index.php?title=Main_Page). Accessed: 2018-04-10.
84. Glut. <https://www.opengl.org/resources/libraries/glut/>. Accessed: 2018-04-10.
85. Leap motion. <https://www.leapmotion.com/>. Accessed: 2018-04-15.

## VITA

NAME	Martina Berni
ADDRESS	1910 N Mozart St, Chicago, IL, 60647 Via A. Caprari 32, Carpi (Mo), Italy, 41012
PHONE	+1 3123585115 +39 3400512867
EMAIL	mberni3@uic.edu martina.berni@mail.polimi.it

---

### EDUCATION

MAR 2017 - <i>In Progress</i>	MASTER OF SCIENCE IN BIOENGINEERING <b>University of Illinois at Chicago</b> , Chicago, USA MASTER THESIS: "Haptic surgical guidance for prostate biopsy" at Mixed Reality Lab, in collaboration with the Department of Urology. Advisor: Cristian Luciano.
OCT 2016 - <i>In Progress</i>	MASTER OF SCIENCE IN BIOENGINEERING Specialization in TECHNOLOGIES FOR ELECTRONICS <b>Politecnico di Milano</b> , Milano, IT
OCT 2013 - JUL 2016	BACHELOR'S DEGREE IN BIOENGINEERING <b>Politecnico di Milano</b> , Milano, IT 109/110 FINAL PROJECT: "Redundancy Optimization of a serial 7 DoF robotic arm" at NearLab. Advisor: Elena De Momi.

---

### RESEARCH EXPERIENCES

JAN 2018 - <i>In Progress</i>	GRADUATE RESEARCH FELLOW <b>Department of Urology, UIC</b> , Chicago, USA
AUG 2017 - <i>In Progress</i>	MASTER THESIS STUDENT <b>Mixed Reality Lab, UIC</b> , Chicago, USA
AUG 2017 - <i>In Progress</i>	MASTER THESIS STUDENT <b>UR*Lab, UIC Innovation Center</b> , Chicago, USA
MAR 2016 - JUL 2016	MASTER THESIS STUDENT <b>NearLab, Politecnico di Milano</b> , Milano, IT

---

## VITA (continued)

---

### LANGUAGE SKILLS

Italian	Native speaker
English	Fluent (IELTS Overall band score 7)

---

### SCHOLARSHIPS

Spring 2018	Graduate Research Assistantship (RA) position (20 hours/week) with full tuition waiver and monthly stipend at UIC
2017/2018	Tuition waiver for high academic performance at Politecnico di Milano
2016/2017	Tuition waiver for high academic performance at Politecnico di Milano
2015/2016	Tuition waiver for high academic performance at Politecnico di Milano
2014/2015	Tuition waiver for high academic performance at Politecnico di Milano
2013/2015	Tuition waiver for high academic performance at Politecnico di Milano

---

### TECHNICAL SKILLS

Base level	3DS Max
Average level	R, Arduino, VolView, Paraview, ITK-SNAP, Slicer3D,, OpenBCI, V-rep, JAVA, OpenGL
Advanced level	MATLAB, Simulink, OpenHaptics, Processing, SolidWorks, C, C++

---

### WORK EXPERIENCE AND PROJECTS

Aug-Dec 2017	<p><i>Binary Input Brain Computer Interface (BCI) based on mu-waves</i></p> <p>Creation of a protocol to collect of EEG signals through OpenBCI, while performing simple motor tasks.</p> <p>Processing of the recorded signal using Matlab in order to recognize mu-waves desynchronization and development of a user interface.</p> <p>Wrote a report including all the technical elements regarding both the hardware and the software.</p>
Mar-Jun 2017	<p><i>Dance, dance revolution, for fingers!</i></p> <p>Built a finger-size prototype of the game using carbon black sheets (capacitive sensors) and an Arduino microprocessor.</p> <p>Programmed the user interface through Processing (Java).</p> <p>Wrote a report including all the technical elements regarding both the hardware and the software.</p>

**VITA (continued)**

Mar-Jun 2016	<i>Redundancy optimization of a serial 7 DoF robotic arm</i> Optimization of Kuka LWR4+ to achieve a more human-like movement. Collection of data from human movement using <i>Microsoft Kinect</i> . Determination of the best DH-parameters for the robot and simulation using V-Rep.
-----------------	---

---